

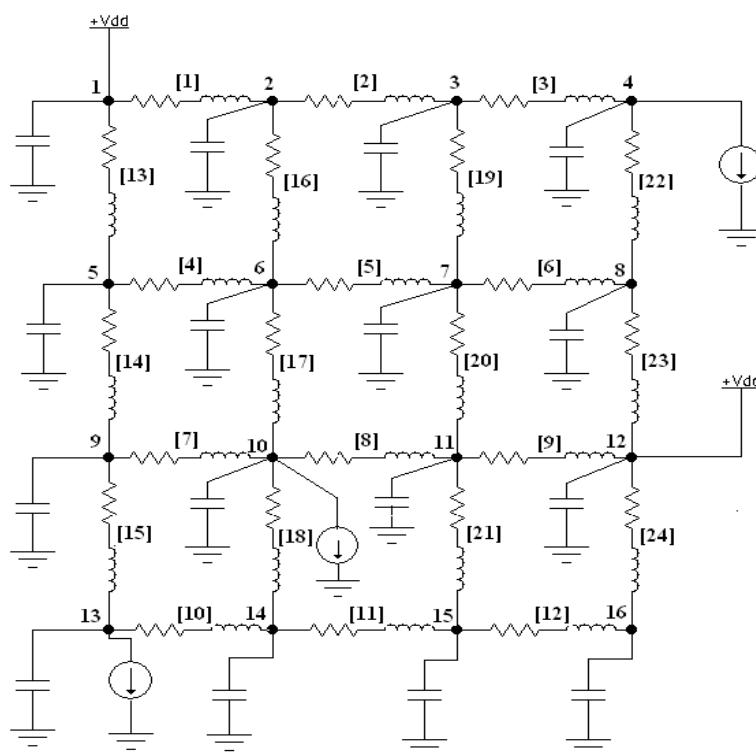
ΠΑΝΕΠΙΣΤΗΜΙΟ ΘΕΣΣΑΛΙΑΣ – ΠΟΛΥΤΕΧΝΙΚΗ ΣΧΟΛΗ
ΤΜΗΜΑ ΜΗΧΑΝΙΚΩΝ Η/Υ ΤΗΛΕΠΙΚΟΙΝΩΝΙΩΝ ΚΑΙ ΔΙΚΤΥΩΝ

ΠΡΟΓΡΑΜΜΑ ΜΕΤΑΠΤΥΧΙΑΚΩΝ ΣΠΟΥΔΩΝ

ΜΕΤΑΠΤΥΧΙΑΚΗ ΕΡΓΑΣΙΑ

Ράμμου Μαρία-Αικατερίνη

Βέλτιστος Σχεδιασμός του Δικτύου Τροφοδοσίας Ολοκληρωμένων Κυκλωμάτων υπό Συνθήκες Δυναμικής Λειτουργίας



Εκπονήθηκε υπό την επίβλεψη των:
Ευμορφόπουλου Νέστορα
Σταμούλη Γεώργιου
Μούντανου Ιωάννη

Βόλος, Απρίλιος 2010

Στους γονείς μου
και τα αδέρφια μου

ΠΕΡΙΕΧΟΜΕΝΑ

I. INTRODUCTION.....	7
II. MODEL AND TRANSIENT ANALYSIS OF THE POWER GRID.....	9
III. STATEMENT OF THE PROBLEMS OF POWER GRID VERIFICATION AND OPTIMIZATION	13
A. Verification problem.....	13
B. Optimization Problem.....	13
IV. DETERMINATION OF THE WORST-CASE CURRENT EXCITATIONS.....	16
A. Instantaneous and cycle-mean voltage drop as function of the excitation waveform	16
B. Maximizers of a linear (or linear affine) function with nonnegative coefficients.....	17
C. Nonnegativity of the coefficients of the voltage drop function in the case of general RLC grid models	19
D. Extension in the case of mutual inductances.....	24
V. DEVELOPMENT OF A PRACTICAL POWER GRID VERIFICATION METHODOLOGY.....	29

VI. FLOW OF THE ALGORITHM AND COMPLEX ANALYSIS.....	32
VII. EXPERIMENTAL TESTS AND RESULTS.....	36
APPENDIX A. PROOFS OF THE THEOREMS.....	41
APPENDIX B. MATLAB CODE.....	49
B.1 Minimize area.....	49
B.1.1 Create waveforms for currents of the input file and find current nodes and voltage nodes.....	49
B.1.2 Find movement vector and maximal points.....	50
B.1.3 Constraint function (gconstr).....	52
B.1.4 Objective function (gridarea)	56
B.1.5 Initialization of the variables and optimization of the grid.....	56
B.2 Minimize noise (Voltage drop).....	58
B.2.1 Create waveforms for currents of the input file and find current nodes and voltage nodes.....	58
B.2.2 Find movement vector and maximal points.....	59
B.2.3 Objective function (gridnoise)	62
B.2.4 Initialization of the variables and optimization of the grid.....	65
REFERENCES.....	68

ΠΕΡΙΛΗΨΗ

Η μείωση της πτώσης τάσης σε ένα δίκτυο διανομής ισχύος είναι ένα από τα μεγαλύτερα προβλήματα αξιοπιστίας για τα σημερινά κυκλώματα VLSI. Τα κελιά και οι ομάδες των λογικών πυλών απορροφούν μεγάλες ποσότητες ρεύματος οι οποίες προκαλούν πτώση τάσης και επαγωγικό θόρυβο στο δίκτυο διανομής ισχύος (grid noise).

Για να αντιμετωπιστούν αυτά τα προβλήματα πρέπει να ικανοποιείται η ευστάθεια (robustness) του δικτύου διανομής ισχύος. Αυτό σημαίνει πως η τάση πρέπει να διατηρείται σε ένα ασφαλές επίπεδο. Δηλαδή, να μην πέφτει κάτω από ένα κατώφλι π.χ. κάτω από το 10% της αρχικής τάσης (10% VDD). Αυτό το πρόβλημα αναφέρεται ως έλεγχος της ακεραιότητας τροφοδοσίας και της ευστάθειας του δικτύου διανομής ισχύος (grid verification) και είναι το ένα από τα δύο προβλήματα που αναλύονται στην παρούσα εργασία.

Το δεύτερο πρόβλημα αναφέρεται ως πρόβλημα βελτιστοποίησης του δικτύου διανομής ισχύος (grid optimization) και έχει να κάνει με την ελαχιστοποίηση της επιφάνειας που καταλαμβάνει το δίκτυο (grid area) ή με την ελαχιστοποίηση του θορύβου του δικτύου (grid noise). Ως grid area ορίζουμε την επιφάνεια που καταλαμβάνουν οι οριζόντιες και οι κάθετες γραμμές τροφοδοσίας καθώς και οι πυκνωτές αποσύζευξης. Ως grid noise ορίζουμε το άθροισμα των ολοκληρωμάτων της πτώσης τάσης, σε όλους τους κόμβους του δικτύου, όταν αυτή βρίσκεται κάτω από ένα επιτρεπτό κατώφλι.

Η βελτιστοποίηση αρχικά ορίζεται έχοντας ως αντικειμενική συνάρτηση την επιφάνεια του δικτύου διανομής ισχύος, η οποία πρέπει να ελαχιστοποιηθεί, υπό τους περιορισμούς των δεδομένων μεγεθών των πλατών των γραμμών τροφοδοσίας και των μηκών των πυκνωτών αποσύζευξης καθώς και της διατήρησης της πτώσης τάσης σε επιτρεπτά επίπεδα, ως ανεξάρτητες παραμέτρους. Στη συνέχεια, η βελτιστοποίηση ορίζεται έχοντας ως αντικειμενική συνάρτηση το θόρυβο, ο οποίος πρέπει να ελαχιστοποιηθεί, υπό τους περιορισμούς των δεδομένων μεγεθών των πλατών των

γραμμών τροφοδοσίας και των μηκών των πυκνωτών αποσύζευξης, ως ανεξάρτητες παραμέτρους.

Η παρούσα εργασία οργανώνεται ως εξής: Στο 2^ο κεφάλαιο γίνεται η δημιουργία και η ανάλυση του δικτύου διανομής ισχύος με βάση την τροποποιημένη μέθοδο των κόμβων (Modified Nodal Analysis) και στο 3^ο αναλύονται τα προβλήματα του ελέγχου της ακεραιότητας του δικτύου και της βελτιστοποίησης του δικτύου διανομής ισχύος. Στο 4^ο κεφάλαιο υπολογίζονται οι χειρότερες πτώσεις τάσης σε κάθε κύκλο ρολογιού για όλους τους κόμβους του δικτύου, υπολογίζοντας πρώτα τις πτώσεις τάσης στα μεγιστικά σημεία (maximal points). Στο 5^ο κεφάλαιο γίνεται ανάπτυξη μιας πρακτική μεθοδολογίας για grid verification ενώ στο επόμενο κεφάλαιο (6^ο) αναλύεται η συνολική ροή του αλγορίθμου. Στο 7^ο κεφάλαιο βρίσκονται τα πειραματικά αποτελέσματα από την προσομοίωση ορισμένων κυκλωμάτων εφαρμόζοντας τις μεθόδους που παρουσιάζονται στην εργασία και για να επιβεβαιωθούν τα αποτελέσματα, έγινε στατιστική ανάλυση ακραίων τιμών. Υπάρχει ξεχωριστό κεφάλαιο με τις αποδείξεις των θεωρημάτων που χρησιμοποιήθηκαν καθώς και ξεχωριστό κεφάλαιο με τον κώδικα που αναπτύχθηκε.

Η εκπόνηση της εργασίας αυτής δε θα ήταν δυνατή χωρίς τη συμβολή, βοήθεια και συμπαράσταση του επιβλέποντα καθηγητή κ. Ευμορφόπουλου Νέστορα καθώς και των καθηγητών κ. Σταμούλη Γεώργιου και κ. Μούντανο Ιωάννη τους οποίους θέλω να ευχαριστήσω θερμά.

I. INTRODUCTION

The deterioration of the voltage level supplied on the active cells or modules by the lines of the power distribution network (voltage-drop or IR-drop) constitutes one of the biggest reliability problems in modern nanometer-scale VLSI circuits. Excessive currents drawn by the active modules and flowing through the finite resistance of the power distribution lines cause substantial voltage drops at the modules and adversely affect circuit speed and noise margins [1]-[2]. Upcoming generations of ICs are going to experience even greater voltage drops (due to increased currents and parasitics), which combined to the reduced supply levels (and increased drop-to-supply ratios) will make the situation extremely harsh.

To get around these problems designers need to have the ability to check if a given power grid is *robust*, i.e. if it constantly maintains a safe voltage level at all active modules under all possible loading conditions. This is commonly referred to as the power grid *verification* problem. In the unfortunate situation, however, where a certain power grid fails to pass a robustness check, there will typically ensue a long and tedious process of tweaking the sizes of power lines and re-checking (under the same circuit loading) until robustness is reached. A common practice is to try over-designing the grid and its lines (i.e. draw them with excessive sizes) at the outset, in an effort to suppress their resistance. However, such an overdesign is in direct conflict with the ever increasing stake of signal lines in routing resources, especially in the less resistive upper metal layers. Besides, since the voltage drop effect is further exacerbated with each new generation of ICs, one cannot tell anymore if a specific design is classified as overdesign or is in fact underdesign. In such cases where an initial robust as well as area-efficient design is dubious, there is need for a systematic methodology that gives the minimum-area grid which satisfies the robustness specifications. This is referred to as the power grid *optimization* (or optimum design) problem. Such a problem is naturally formulated as a constrained optimization problem where the grid area is an objective function to be minimized with respect to the widths of the power lines and the lengths of the decoupling capacitors (as independent variables) and under constraints on voltage drop at all active modules [20], [22]. It is also formulated as a constrained optimization problem where noise (a

sum of the integrals of the voltage drop in the nodes where it remains below a user specified noise ceiling) is an objective function to be minimized with respect to the widths of the power lines and the lengths of the decoupling capacitors (as independent variables) [21]. The constraints arise from an explicit network analysis which expresses the voltage drops at the modules as function of the independent variable widths with one or more vectors of current excitations from these modules (denoted as current sources). Most recent attempts [3]-[5] were based on a modification of the above framework proposed some years ago [6] in which two sets of independent variables (branch currents and node voltages) were employed instead of the single set of branch widths, and the network - current and voltage - laws were taken as additional constraints (effectively performing an implicit network analysis within the optimization algorithm). This was done in order to relax the original problem and solve it in two steps (by successively fixing one set of parameters at each step) involving a convex programming and a linear programming problem, both of which can be solved efficiently by known methods in the literature. However, there are several important problems and shortcomings with the aforementioned modification. First of all, the relaxation process does not actually solve the original problem but its relaxed counterpart, a fact that inevitably introduces inaccuracies in the final solution. Without the relaxation process the problem is no more than a nonlinear programming problem, which is also characterized by an almost twofold increase in the number of optimization parameters along with hundreds (or thousands) of additional constraints emerging from the network laws. The greatest problem, however, with the modified framework is that since node voltages and branch currents are selected as unknown parameters for optimization, only one set of current waveform excitations can be specified which finally produce those unknown currents and voltages. Also, since the output of the simulation for the sink currents is a function of the sequence of input patterns applied on the digital circuit, to fully check grid robustness or build a complete set of constraints one has to enumerate all possible input patterns, which is clearly impractical.

II. MODEL AND TRANSIENT ANALYSIS OF THE POWER GRID

As already stated, we will be concerned with the full RLC model of the power grid. Let the power grid be composed of b branches and $n + p$ nodes, of which p nodes are connected to the external power supply via power pads, and the remaining n nodes are divided to m sink nodes (with current sources to an external ground node) and $n - m$ internal nodes.

Due to the presence of both C and L elements in a full RLC model, we will employ the Modified Nodal Analysis (MNA) – instead of the standard Nodal Analysis – for the analysis of the power grid, wherein inductor currents constitute additional variables alongside node voltages. Especially for networks representing power grids we typically model each wire segment (between two contacts) as a resistance in series with an inductance, with capacitances to ground at the two contact nodes (Fig. 1). Thus, in the analysis that follows we will consider the b branches of the grid as *composite* resistive-inductive (R-L) branches.

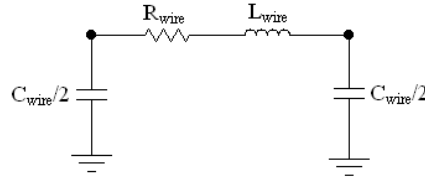


Fig. 1. Typical model of a wire segment in power grids.

The Kirchhoff's current and voltage laws for the linear network representing the power grid are as follows:

$$\text{KCL: } \begin{bmatrix} \mathbf{A}_{rl} & \mathbf{A}_c \end{bmatrix} \begin{bmatrix} \mathbf{i}_b(t) \\ \mathbf{i}_c(t) \end{bmatrix} = \mathbf{e}_n(t), \text{ or}$$

$$(1) \quad \mathbf{A}_{rl} \mathbf{i}_b(t) + \mathbf{i}_c(t) = \mathbf{e}_n(t)$$

$$\text{KVL: } \begin{bmatrix} \mathbf{A}_{rl}^T \\ \mathbf{A}_c^T \end{bmatrix} \mathbf{v}_n(t) = \begin{bmatrix} \mathbf{v}_b(t) \\ \mathbf{v}_c(t) \end{bmatrix}, \text{ or}$$

$$(2a) \quad \mathbf{A}_{rl}^T \mathbf{v}_n(t) = \mathbf{v}_b(t)$$

$$(2b) \quad \mathbf{v}_n(t) = \mathbf{v}_c(t)$$

In the above, \mathbf{A}_{rl} is the $n \times b$ incidence matrix of the directed composite R-L branches (with arbitrary reference directions), whose elements are defined as follows:

$$a_{ij} = \begin{cases} +1, & \text{when direction of branch } j \text{ is away from node } i \\ -1, & \text{when direction of branch } j \text{ is towards node } i \\ 0, & \text{when branch } j \text{ is not incident with node } i \end{cases}$$

Furthermore, $\mathbf{v}_n(t)$, $\mathbf{v}_b(t)$, and $\mathbf{i}_b(t)$ are the $n \times 1$, $b \times 1$, and $b \times 1$ vectors of node voltages, branch voltages, and branch currents respectively, $\mathbf{e}_n(t)$ is a $n \times 1$ vector of excitations from independent sources (either current or voltage ones) at the nodes, $\mathbf{i}_c(t)$ is a $n \times 1$ vector of currents of the additional capacitive branches which appear at the n nodes, and \mathbf{A}_c is the $n \times n$ incidence matrix of those n branches, for which $\mathbf{A}_c = \mathbf{I}_n$ (the $n \times n$ identity matrix) since all capacitive branches are directed away from the nodes and are connected to ground.

The current-voltage relationships of the n capacitive branches and the b composite R-L branches are as follows:

$$(3) \quad \mathbf{i}_c(t) = \mathbf{C}_n \dot{\mathbf{v}}_c(t) = \mathbf{C}_n \dot{\mathbf{v}}_n(t)$$

$$(4) \quad \mathbf{v}_b(t) = \mathbf{R}_b \mathbf{i}_b(t) + \mathbf{L}_b \dot{\mathbf{i}}_b(t)$$

where $\dot{\mathbf{v}}_n(t)$ and $\dot{\mathbf{i}}_b(t)$ are the time derivatives of vectors $\mathbf{v}_n(t)$ and $\mathbf{i}_b(t)$ respectively, \mathbf{C}_n is a $n \times n$ diagonal matrix of the node capacitances, and \mathbf{R}_b , \mathbf{L}_b are $b \times b$ matrices of the resistances and inductances of the composite R-L branches. The

matrix \mathbf{R}_b is a diagonal matrix, while \mathbf{L}_b is either diagonal if there are only self-inductances at the branches, or a full matrix if there are also mutual inductances between branches. We assume that each R-L branch has nonzero self-inductance and each node has nonzero capacitance, so that the matrices \mathbf{L}_b and \mathbf{C}_n are nonsingular (invertible).

In MNA we replace (3) into (1), and (4) into (2a), in order to obtain the following system of first-order differential equations (with respect to $\mathbf{v}_n(t)$ and $\mathbf{i}_b(t)$):

$$(5) \quad \mathbf{A}_{rl} \mathbf{i}_b(t) + \mathbf{C}_n \dot{\mathbf{v}}_n(t) = \mathbf{e}_n(t)$$

$$(6) \quad \mathbf{R}_b \mathbf{i}_b(t) + \mathbf{L}_b \dot{\mathbf{i}}_b(t) - \mathbf{A}_{rl}^T \mathbf{v}_n(t) = \mathbf{0}$$

If we write the variable vectors $\mathbf{v}_n(t)$ and $\mathbf{i}_b(t)$ as the new vector $\mathbf{x}(t) = \begin{bmatrix} \mathbf{v}_n(t) \\ \mathbf{i}_b(t) \end{bmatrix}$ we

can write the systems of equations (5) and (6) as the new system:

$$(7) \quad \tilde{\mathbf{G}} \mathbf{x}(t) + \tilde{\mathbf{C}} \dot{\mathbf{x}}(t) = \mathbf{e}(t)$$

$$\text{where } \tilde{\mathbf{G}} = \begin{bmatrix} \mathbf{0} & \mathbf{A}_{rl} \\ -\mathbf{A}_{rl}^T & \mathbf{R}_b \end{bmatrix}, \tilde{\mathbf{C}} = \begin{bmatrix} \mathbf{C}_n & \mathbf{0} \\ \mathbf{0} & \mathbf{L}_b \end{bmatrix}, \mathbf{e}(t) = \begin{bmatrix} \mathbf{e}_n(t) \\ \mathbf{0} \end{bmatrix}.$$

In the above system $\mathbf{v}_n(t)$ is the vector of node voltages, but the system is easily re-expressed with respect to the *voltage drops* at the nodes by omitting the independent voltage sources in the excitation vector $\mathbf{e}_n(t)$ and reversing the sign of the current sources (from $-$ to $+$). From now on we will denote $\mathbf{v}_n(t)$ as the vector of voltage drops at the nodes.

We remark here that in the optimization problem the matrix of node capacitances (\mathbf{C}_n) as well as the matrices of the resistances and inductances of the composite R-L branches (\mathbf{R}_b and \mathbf{L}_b respectively) are no longer constant but depend on decap lengths (\mathbf{l}) and wire widths (\mathbf{w}) and should be written as $\mathbf{C}_n(\mathbf{w}, \mathbf{l})$, $\mathbf{R}_b(\mathbf{w}, \mathbf{l})$ and $\mathbf{L}_b(\mathbf{w}, \mathbf{l})$.

By the Backward Euler differential approximation for a fixed time step h , we can replace the time derivative $\dot{\mathbf{x}}(t)$ with its finite difference formula $\dot{\mathbf{x}}(t) \approx \frac{\mathbf{x}(t) - \mathbf{x}(t-h)}{h}$ in (7) and obtain $(\tilde{\mathbf{G}} + \tilde{\mathbf{C}}/h)\mathbf{x}(t) = (\tilde{\mathbf{C}}/h)\mathbf{x}(t-h) + \mathbf{e}(t)$ for $t = kh$, $k = 1, 2, \dots$, or:

$$(8) \quad \begin{aligned} \mathbf{x}(kh) &= (\tilde{\mathbf{G}} + \tilde{\mathbf{C}}/h)^{-1} \mathbf{e}(kh) + (\tilde{\mathbf{G}} + \tilde{\mathbf{C}}/h)^{-1} (\tilde{\mathbf{C}}/h) \mathbf{x}((k-1)h) \\ &\equiv \mathbf{B}_1 \mathbf{e}(kh) + \mathbf{B} \mathbf{x}((k-1)h) \end{aligned}$$

where $\mathbf{B}_1 = (\tilde{\mathbf{G}} + \tilde{\mathbf{C}}/h)^{-1}$ and $\mathbf{B} = (\tilde{\mathbf{G}} + \tilde{\mathbf{C}}/h)^{-1} (\tilde{\mathbf{C}}/h) = \mathbf{B}_1 (\tilde{\mathbf{C}}/h)$.

The latter recursive relation is used to calculate all node voltage drops and all branch currents at a particular time instant $t = kh$, $k = 1, 2, \dots$ based on the voltage drops and branch currents at the previous time instant $t = (k-1)h$.

III. STATEMENT OF THE PROBLEMS OF POWER GRID VERIFICATION AND OPTIMIZATION

A. Verification Problem

The process of power grid verification typically involves checking that the maximum voltage drop at all sink nodes, under all possible transient current waveforms, does not exceed a safety threshold voltage v_o (e.g. $v_o = 0.1V_{dd}$) at all time instants t :

$$v_s(t) < v_o, \forall t \in \mathfrak{R}.$$

Since the latter is equivalent to $\max_{t \in \mathfrak{R}} v_s(t) < v_o$ (where the “max” operator is interpreted component-wise in vector $v_s(t)$), we need to find the maximum voltage drop $\max_{t \in \mathfrak{R}} v_k(t)$ at each sink $1 \leq k \leq n$.

B. Optimization Problem

In the optimization problem we seek to minimize the objective function of the area which is the sum of the area of horizontal wires, the area of vertical wires and the area of the decoupling capacitors. We assume that decoupling capacitors are square blocks. The optimization is subject to keeping noise (voltage drop) in every grid node less than a threshold value (10% Vdd) and keeping wire widths and decoupling capacitors lengths between reasonable bounds.

$$\textbf{Minimize} \quad Area(\mathbf{w}, \mathbf{l}) = L_h \sum_{i=1}^{b_h} w_i + L_v \sum_{j=1}^{b_v} w_j + \sum_{k=1}^{ndec} l_k^2$$

$$\textbf{Subject to} \quad \max_{t \in \mathfrak{R}} v_s(t) < v_o \quad \text{Optimization Problem (1)}$$

$$\textbf{and} \quad w_{\min} \leq w_i \leq w_{\max}, \quad l_{\min} \leq l \leq l_{\max}$$

Where L_h is the length of horizontal wires, L_v is the length of vertical wires, w is the width of a wire, b_h is the number of horizontal branches, b_v is the number of vertical branches, l is the length of the decoupling capacitors and $ndec$ is the number of the decoupling capacitors, which in our case is equal to the number of nodes.

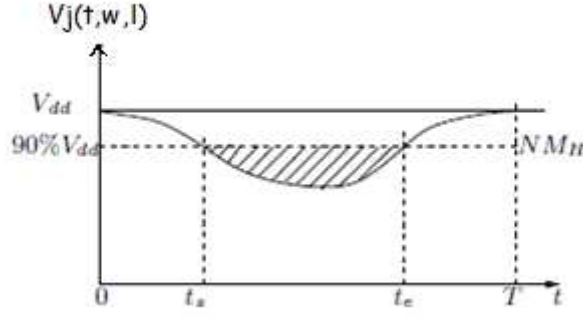


Fig. 2. Voltage waveform of one node on the Vdd grid.

Another formulation of the optimization problem is minimizing noise. Noise at a node can be efficiently measured using the integral of the voltage drop below a user specified noise ceiling as:

$$Z_j(\mathbf{w}, \mathbf{l}) = \int_0^T \max\{NM_H - v_j(t, \mathbf{w}, \mathbf{l}), 0\} = \int_{t_s}^{t_e} \{NM_H - v_j(t, \mathbf{w}, \mathbf{l})\} dt$$

where (\mathbf{w}, \mathbf{l}) represent the tunable circuit parameters which, in our case, are the widths of the power grid wires and the lengths of the decoupling capacitors (supposing decoupling capacitors are square). This idea is pictorially illustrated in the above figure, which shows the voltage waveform of one node on the Vdd grid.

The noise metric for the entire circuit (which is now the objective function) is defined as the (possibly weighted) sum of all of the individual node metrics:

$$Z = \sum_{j=1}^K z_j(\mathbf{w}, \mathbf{l})$$

K is the number of nodes. This metric penalizes more harshly transients that exceed the imposed noise ceiling by a large amount for a long time, and has empirically been seen to be more effective in practice than one that penalizes merely the maximum

noise violation. Intuitively, this can be explained by the fact that the metric incorporates, in a sense, both the voltage and time axes together, as well as spatial considerations through the summation over all nodes in the circuit. The optimization now is subject to keeping wire widths and decoupling capacitors lengths between reasonable bounds.

The optimization problem can be formulated as:

$$\textbf{Minimize} \quad Z = \sum_{j=1}^K z_j(\mathbf{w}, \mathbf{l})$$

$$\textbf{Subject to} \quad w_{\min} \leq w_i \leq w_{\max}, \quad l_{\min} \leq l \leq l_{\max} \quad \text{Optimization Problem (2)}$$

IV. DETERMINATION OF THE WORST-CASE CURRENT EXCITATIONS

A. Instantaneous and cycle-mean voltage drop as function of the excitation waveforms

Both for the verification and the optimization problem we seek to find all current waveforms that constitute worst-case waveforms, in the sense that they produce the worst voltage drop during a clock cycle.

By successive substitutions of the recursive expressions for $\mathbf{x}((k-1)h)$, $\mathbf{x}((k-2)h)$, \dots , $\mathbf{x}(h)$ into (8) we obtain:

$$\begin{aligned}\mathbf{x}(kh) &= \mathbf{B}_1 \mathbf{e}(kh) + \mathbf{B} \mathbf{B}_1 \mathbf{e}((k-1)h) + \dots + \mathbf{B}^{k-1} \mathbf{B}_1 \mathbf{e}(h) + \mathbf{B}^k \mathbf{x}(0) \\ &= \sum_{j=0}^{k-1} \mathbf{B}^j \mathbf{B}_1 \mathbf{e}((k-j)h) + \mathbf{B}^k \mathbf{x}(0), \quad k=1,2,\dots\end{aligned}$$

However, both for timing and noise purposes, the peak instantaneous voltage drop is not as important as the integral of voltage drop (or the mean voltage drop) within a specified time interval $T = Nh$, which may be equal or smaller than the clock period – e.g. an interval of high activity within the clock cycle (a large instantaneous voltage drop will not severely affect timing but a large cumulative voltage drop over a time interval will). The mean vector of voltage drops and branch currents within such an interval is:

$$\begin{aligned}\bar{\mathbf{x}} &= \frac{1}{Nh} [\mathbf{x}(h) + \mathbf{x}(2h) + \dots + \mathbf{x}(Nh)] = \\ &= \frac{1}{Nh} [\mathbf{B}_1 \mathbf{e}(Nh) + (\mathbf{I} + \mathbf{B}) \mathbf{B}_1 \mathbf{e}((N-1)h) + \dots + (\mathbf{I} + \mathbf{B} + \dots + \mathbf{B}^{N-1}) \mathbf{B}_1 \mathbf{e}(h) + \mathbf{c}] \text{ where} \\ \mathbf{c} &\equiv (\mathbf{B} + \mathbf{B}^2 + \dots + \mathbf{B}^N) \mathbf{x}(0).\end{aligned}$$

Since $\mathbf{B}_1 = h\mathbf{B}\tilde{\mathbf{C}}^{-1}$ (where $\tilde{\mathbf{C}}^{-1} = \begin{bmatrix} \mathbf{C}_n^{-1} & \mathbf{0} \\ \mathbf{0} & \mathbf{L}_b^{-1} \end{bmatrix}$) we have $\mathbf{B}_1 \mathbf{e}(kh) = h\mathbf{B}\mathbf{e}_c(kh)$

(where $\mathbf{e}_c(kh) \equiv \begin{bmatrix} \mathbf{C}_n^{-1} \mathbf{e}_n(kh) \\ \mathbf{0} \end{bmatrix}$) for each $k = 1, 2, \dots, N$, so

$$\bar{\mathbf{x}} = \frac{1}{N} [\mathbf{B} \mathbf{e}_c(Nh) + (\mathbf{B} + \mathbf{B}^2) \mathbf{e}_c((N-1)h) + \dots + (\mathbf{B} + \mathbf{B}^2 + \dots + \mathbf{B}^N) \mathbf{e}_c(h) + \mathbf{c}]$$

By denoting the upper-left $n \times n$ blocks of the matrices \mathbf{B} , $\mathbf{B} + \mathbf{B}^2, \dots$, $\mathbf{B} + \mathbf{B}^2 + \dots + \mathbf{B}^N$ as $(\mathbf{B})_{n \times n}$, $(\mathbf{B} + \mathbf{B}^2)_{n \times n}, \dots$, $(\mathbf{B} + \mathbf{B}^2 + \dots + \mathbf{B}^N)_{n \times n}$, we have for the block $\bar{\mathbf{v}}_n$ of voltage drops within the vector $\bar{\mathbf{x}}$:

$$\begin{aligned} (9) \quad \bar{\mathbf{v}}_n &= \frac{1}{N} [(\mathbf{B})_{n \times n} \mathbf{C}_n^{-1} \mathbf{e}_n(Nh) + (\mathbf{B} + \mathbf{B}^2)_{n \times n} \mathbf{C}_n^{-1} \mathbf{e}_n((N-1)h) + \\ &\quad + \dots + (\mathbf{B} + \mathbf{B}^2 + \dots + \mathbf{B}^N)_{n \times n} \mathbf{C}_n^{-1} \mathbf{e}_n(h) + \mathbf{c}_{n \times 1}] \\ &\equiv \frac{1}{N} [(\mathbf{B})_{n \times n} \mathbf{C}_n^{-1} \mathbf{e}_N + (\mathbf{B} + \mathbf{B}^2)_{n \times n} \mathbf{C}_n^{-1} \mathbf{e}_{N-1} + \dots + (\mathbf{B} + \mathbf{B}^2 + \dots + \mathbf{B}^N)_{n \times n} \mathbf{C}_n^{-1} \mathbf{e}_1 + \mathbf{c}_{n \times 1}] \end{aligned}$$

where we have written the vectors of excitations $\mathbf{e}_n(Nh)$, $\mathbf{e}_n((N-1)h), \dots, \mathbf{e}_n(h)$ at time instants $t = kh, k = 1, 2, \dots, N$ as $\mathbf{e}_N, \mathbf{e}_{N-1}, \dots, \mathbf{e}_1$ since we will treat them as variables hereafter. Thus we have arrived at the result that the mean voltage drop at each node $i = 1, 2, \dots, n$ (i.e. each component \bar{v}_i , $i = 1, 2, \dots, n$ within $\bar{\mathbf{v}}_n$) is a linear function (or a linear affine function if the constant vector \mathbf{c} is not $\mathbf{0}$) of the super-vector of $M \equiv mN$ dimensions:

$$\mathbf{y} \equiv (e_{N,1}, e_{N,2}, \dots, e_{N,m}, e_{N-1,1}, e_{N-1,2}, \dots, e_{N-1,m}, \dots, e_{1,1}, e_{1,2}, \dots, e_{1,m})$$

which consists of the (discretized) current waveform excitations at the m sink nodes (we remind that in each $n \times 1$ vector $\mathbf{e}_N, \mathbf{e}_{N-1}, \dots, \mathbf{e}_1$ only m of the n components that correspond to sink nodes are nonzero).

B. Maximizers of a linear (or linear affine) function with nonnegative coefficients

The variable vector \mathbf{y} in every function $\bar{v}_i \equiv \bar{v}_i(\mathbf{y})$, $i = 1, 2, \dots, n$ does not attain all values in the M -dimensional space $\Re^M \equiv \Re^{mN}$. Instead, the excitation values at each

sink $j = 1, 2, \dots, m$ and at each time instant $t = kh, k = 1, 2, \dots, N$ depend on the specific clock cycle where they are considered, i.e. on the pair of binary vectors $\{\mathbf{b}_p, \mathbf{b}_n\}$ being applied on the digital circuit before and after the clock edge. This means that the vector \mathbf{y} is actually a vector-valued function $\mathbf{y} \equiv \mathbf{y}(\{\mathbf{b}_p, \mathbf{b}_n\})$ whose range of values $D \subset \mathfrak{R}^M$ constitutes the *domain* on which the linear function $\bar{v}_i(\mathbf{y})$ is defined. This domain D (henceforth referred to as the “excitation space”) is obviously bounded (since the drawn currents at every time instant are all finite) and closed (since it contains its boundary points), which means that it is a *compact* set of \mathfrak{R}^M . Due to the well-known Weierstrass theorem [7], a continuous function $f(\mathbf{y})$ defined on a compact set $D \subset \mathfrak{R}^M$ (i.e. $f: D \rightarrow \mathfrak{R}$) always attains a maximum at some point $\mathbf{y}^* \in D$ (maximizing point or maximizer of $f(\mathbf{y})$). Each function $\bar{v}_i(\mathbf{y})$, $i = 1, 2, \dots, n$ is a linear function of \mathbf{y} , and for R or RC grid models it is well known and easy to prove that it has *nonnegative* coefficients in all components of the vector \mathbf{y} (due to the matrix $\tilde{\mathbf{G}} + \tilde{\mathbf{C}}/h$ being inverse-nonnegative in the absence of inductive elements – for general RLC models see next section). We seek to locate the maximizing points $\mathbf{y}^* \in D$ for $\bar{v}_i(\mathbf{y})$ among all $\mathbf{y} \in D$ (i.e. among all possible clock cycles and corresponding binary vector pairs) which can be characterized as the worst-case excitations. For this specific type of function the following hold with respect to its maximizing points:

Definition 1. A point $\mathbf{y} \in D$ is called a *maximal* (or *noninferior*) point of the set $D \subset \mathfrak{R}^M$ if for every $\mathbf{y}' \in D$ the relation $\mathbf{y}' \geq \mathbf{y}$ implies $\mathbf{y}' = \mathbf{y}$, or equivalently if there does not exist a $\mathbf{y}' \in D$ such that $\mathbf{y}' \geq \mathbf{y}$ (component-wise) with at least one component $i = 1, \dots, M$ being $y'_i > y_i$.

Theorem 1. [15] Let $f(\mathbf{y}) = \sum_{i=1}^M a_i y_i = \mathbf{a}^T \cdot \mathbf{y}$ be a linear (or linear affine) function with nonnegative coefficient vector \mathbf{a} (i.e. $\mathbf{a} \geq \mathbf{0}$ component-wise) which is defined on a compact set $D \subset \mathfrak{R}^M$. If $\mathbf{y}^* \in D$ is a maximizer of $f(\mathbf{y})$ [i.e. $f(\mathbf{y}^*) = \max_{\mathbf{y} \in D} f(\mathbf{y})$], then \mathbf{y}^* is a maximal point of D .

The above theorem effectively means that in order to find the maximizing points of a linear function $f(\mathbf{y}) = \mathbf{a}^T \cdot \mathbf{y}$ with $\mathbf{a} \geq \mathbf{0}$ which is defined on a closed and bounded set $D \subset \mathbb{R}^M$ we may confine our search to the subset consisting of the maximal points of D (Fig. 3).

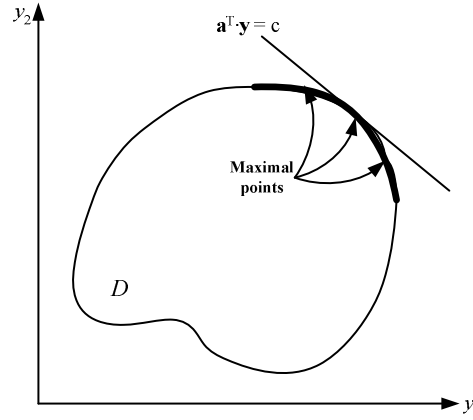


Fig. 3. Maximal points of a compact set $D \subset \mathbb{R}^M$ and maximization of a linear function $f(\mathbf{y}) = \mathbf{a}^T \cdot \mathbf{y}$ over it (only the level line of $f(\mathbf{y})$ at the maximizing point \mathbf{y}^* is shown in the figure – the actual graph of $f(\mathbf{y})$ is a plane in 3 dimensions).

C. Nonnegativity of the coefficients of the voltage drop function in the case of general RLC grid models

In contrast to the case of R or RC grid models, it is not at all obvious whether every mean voltage drop function $\bar{v}_i \equiv \bar{v}_i(\mathbf{y})$ in (9) has nonnegative coefficients, in order for the maximal waveform points to still represent the worst-case excitations.

At first, since all capacitances in the diagonal matrix \mathbf{C}_n are positive, the matrix \mathbf{C}_n^{-1} is also positive diagonal and thus it is sufficient to examine the $n \times n$ upper-left blocks $(\mathbf{B})_{n \times n}, (\mathbf{B} + \mathbf{B}^2)_{n \times n}, \dots, (\mathbf{B} + \mathbf{B}^2 + \dots + \mathbf{B}^N)_{n \times n}$ of the matrices $\mathbf{B}, \mathbf{B} + \mathbf{B}^2, \dots, \mathbf{B} + \mathbf{B}^2 + \dots + \mathbf{B}^N$. The matrix \mathbf{B} can be written as:

$$(10) \quad \mathbf{B} = (\tilde{\mathbf{G}} + \tilde{\mathbf{C}}/h)^{-1}(\tilde{\mathbf{C}}/h) = (h\tilde{\mathbf{C}}^{-1}(\tilde{\mathbf{G}} + \tilde{\mathbf{C}}/h))^{-1} = (h\tilde{\mathbf{C}}^{-1}\tilde{\mathbf{G}} + \mathbf{I})^{-1}$$

$$= \begin{bmatrix} \mathbf{I}_n & \mathbf{A}_C \\ -\mathbf{A}_L & \mathbf{I}_b + \mathbf{R}_L \end{bmatrix}^{-1}$$

where $\mathbf{A}_C = h\mathbf{C}_n^{-1}\mathbf{A}_{rl}$, $\mathbf{A}_L = h\mathbf{L}_b^{-1}\mathbf{A}_{rl}^T$, $\mathbf{R}_L = h\mathbf{L}_b^{-1}\mathbf{R}_b$

and \mathbf{I} , \mathbf{I}_n , and \mathbf{I}_b are the $(n+b) \times (n+b)$, $n \times n$, and $b \times b$ identity matrices respectively.

By performing block matrix inversion [8] in (10) we have:

$$(11) \quad \mathbf{B} = \begin{bmatrix} \mathbf{Q} & -\mathbf{Q}\mathbf{A}_C\mathbf{U} \\ \mathbf{U}\mathbf{A}_L\mathbf{Q} & \mathbf{U} - \mathbf{U}\mathbf{A}_L\mathbf{Q}\mathbf{A}_C\mathbf{U} \end{bmatrix}$$

where $\mathbf{U} = (\mathbf{I}_b + \mathbf{R}_L)^{-1}$ and $\mathbf{Q} = (\mathbf{I}_n + \mathbf{A}_C\mathbf{U}\mathbf{A}_L)^{-1}$

(just multiply (11) by $\begin{bmatrix} \mathbf{I}_n & \mathbf{A}_C \\ -\mathbf{A}_L & \mathbf{I}_b + \mathbf{R}_L \end{bmatrix}$ and verify that their product is the $(n+b) \times (n+b)$ identity matrix \mathbf{I}).

For the moment, we will assume only self-inductances in the power grid model so that the matrix \mathbf{L}_b (and \mathbf{L}_b^{-1}) is positive diagonal (we will treat mutual inductances in the next section). With this assumption we can readily show that the upper-left $n \times n$ block $(\mathbf{B})_{n \times n} = \mathbf{Q}$ of \mathbf{B} has only nonnegative elements (i.e. $\mathbf{Q} \geq \mathbf{0}$ element-wise). Indeed, if \mathbf{L}_b is positive diagonal, then $\mathbf{U}h\mathbf{L}_b^{-1} = (\mathbf{I}_b + h\mathbf{L}_b^{-1}\mathbf{R}_b)^{-1}h\mathbf{L}_b^{-1}$ is also positive diagonal, and the product $\mathbf{V} = \mathbf{A}_{rl}(\mathbf{U}h\mathbf{L}_b^{-1})\mathbf{A}_{rl}^T$ where \mathbf{A}_{rl} is an incidence matrix and $\mathbf{U}h\mathbf{L}_b^{-1}$ is a positive diagonal matrix is well known to have the following properties [9]: (i) positive diagonal elements ($v_{ii} > 0$, $i = 1, \dots, n$), (ii) nonpositive off-diagonal elements ($v_{ij} \leq 0$, $i, j = 1, \dots, n$, $i \neq j$), (iii) symmetry ($v_{ij} = v_{ji}$, $i, j = 1, \dots, n$), (iv) diagonal dominance, defined as follows:

Definition 2. A $n \times n$ matrix $\mathbf{V} = [v_{ij}]$ is called *row diagonally dominant* if

$$|v_{ii}| \geq \sum_{\substack{j=1 \\ j \neq i}}^n |v_{ij}|, \quad \forall i = 1, \dots, n.$$

$$\text{if } |v_{jj}| \geq \sum_{\substack{i=1 \\ i \neq j}}^n |v_{ij}|, \quad \forall j = 1, \dots, n.$$

Obviously a symmetric matrix is both row and column diagonally dominant. It is easy, now, to show the following result about symmetric diagonally dominant matrices with positive diagonal elements and nonpositive off-diagonal elements:

Lemma 1. If $\mathbf{V} = [v_{ij}]$ is a $n \times n$ symmetric diagonally dominant matrix with positive diagonal elements and nonpositive off-diagonal elements, and $\mathbf{C} = [c_i]$, $\mathbf{D} = [d_i]$ are $n \times n$ positive and nonnegative diagonal matrices respectively (i.e. $c_i > 0$ and $d_i \geq 0$, $i = 1, \dots, n$), then $\mathbf{W} = \mathbf{D} + \mathbf{CV}$ is a $n \times n$ row diagonally dominant matrix and $\mathbf{Y} = \mathbf{D} + \mathbf{VC}$ is a $n \times n$ column diagonally dominant matrix, both with positive diagonal elements and nonpositive off-diagonal elements (proof in Appendix A).

Because of the above theorem we have that the matrix $\mathbf{I}_n + \mathbf{A}_C \mathbf{U} \mathbf{A}_L = \mathbf{I}_n + h \mathbf{C}_n^{-1} \mathbf{A}_{rl} \mathbf{U} h \mathbf{L}_b^{-1} \mathbf{A}_{rl}^T$ is row diagonally dominant with positive diagonal elements and nonpositive off-diagonal elements. These properties are sufficient for a matrix to be classified as an *M-matrix* [10], which by definition is inverse-nonnegative, i.e. $\mathbf{Q} = (\mathbf{I}_n + \mathbf{A}_C \mathbf{U} \mathbf{A}_L)^{-1} \geq \mathbf{0}$.

For the remaining blocks $(\mathbf{B} + \mathbf{B}^2)_{n \times n}, \dots, (\mathbf{B} + \mathbf{B}^2 + \dots + \mathbf{B}^N)_{n \times n}$ we have that $\mathbf{B} \equiv \mathbf{S}_1$, $\mathbf{B} + \mathbf{B}^2 \equiv \mathbf{S}_2, \dots$, $\mathbf{B} + \mathbf{B}^2 + \dots + \mathbf{B}^N \equiv \mathbf{S}_N$ constitute partial sums of the series $\mathbf{B} + \mathbf{B}^2 + \dots = \mathbf{B}(\mathbf{I} + \mathbf{B} + \dots) = \mathbf{B} \sum_{N=0}^{\infty} \mathbf{B}^N$ which converges to the matrix $\mathbf{B}(\mathbf{I} - \mathbf{B})^{-1} \equiv \mathbf{S}$, on condition that $\lim_{N \rightarrow \infty} \mathbf{B}^N = \mathbf{0}$ [11]. This means that the sequence of the ij th elements $s_{ij}^{(N)}$ of the partial sums \mathbf{S}_N converges to the ij th element s_{ij} of \mathbf{S} for every

$i, j = 1, \dots, n + b$ (i.e. $\lim_{N \rightarrow \infty} s_{ij}^{(N)} = s_{ij}$, $\forall i, j = 1, \dots, n + b$), and this of course is true for the upper-left $n \times n$ elements $s_{ij}^{(N)}$ and s_{ij} , $i, j = 1, \dots, n$. By writing the limit matrix \mathbf{S} via (10) as:

$$(12) \quad \mathbf{S} = \mathbf{B}(\mathbf{I} - \mathbf{B})^{-1} = (\mathbf{B}^{-1} - \mathbf{I})^{-1} = \begin{bmatrix} \mathbf{0} & \mathbf{A}_C \\ -\mathbf{A}_L & \mathbf{R}_L \end{bmatrix}^{-1}$$

we find by block matrix inversion that its $n \times n$ upper-left block is:

$$(13) \quad (\mathbf{S})_{n \times n} = (\mathbf{B}(\mathbf{I} - \mathbf{B})^{-1})_{n \times n} = (\mathbf{A}_C \mathbf{R}_L^{-1} \mathbf{A}_L)^{-1} = (h \mathbf{C}_n^{-1} \mathbf{A}_{rl} \mathbf{R}_b^{-1} \mathbf{A}_{rl}^T)^{-1}$$

The matrix $h \mathbf{C}_n^{-1} \mathbf{A}_{rl} \mathbf{R}_b^{-1} \mathbf{A}_{rl}^T$ is – on account of Lemma 1 – row diagonally dominant with positive diagonal elements and nonpositive off-diagonal elements, and is thus an M-matrix which is inverse-nonnegative, i.e. $(\mathbf{S})_{n \times n} \geq \mathbf{0}$.

Overall, we have a series of matrices which starts off by a first term $\mathbf{S}_1 = \mathbf{B}$ with a nonnegative upper-left $n \times n$ block, accepts additive terms $\mathbf{B}^2, \mathbf{B}^3, \dots$ (to form the intermediate partial sums) which have gradually smaller elements than \mathbf{B} (due to $\lim_{N \rightarrow \infty} \mathbf{B}^N = \mathbf{0}$, which is equivalent to $\lim_{N \rightarrow \infty} \|\mathbf{B}^N\| = 0$ – see in a moment about this), and converges to a limit $\mathbf{S} = \mathbf{B}(\mathbf{I} - \mathbf{B})^{-1}$ with also a nonnegative upper-left $n \times n$ block. This ensures us that all intermediate partial sums $\mathbf{B} + \mathbf{B}^2, \mathbf{B} + \mathbf{B}^2 + \mathbf{B}^3, \dots$ will have nonnegative upper-left $n \times n$ blocks, i.e. $(\mathbf{B} + \mathbf{B}^2)_{n \times n} \geq \mathbf{0}, (\mathbf{B} + \mathbf{B}^2 + \mathbf{B}^3)_{n \times n} \geq \mathbf{0}, \dots$

As a practical example, consider a grid with $n = 6$ nodes and $b = 8$ branches, and the following incidence, node capacitance, branch resistance and branch inductance matrices:

$$\mathbf{A}_{rl} = \begin{bmatrix} 1 & 0 & 0 & 0 & 1 & 0 & 0 & 0 \\ -1 & 1 & 0 & 0 & 0 & 1 & 0 & -1 \\ 0 & -1 & 0 & 0 & 0 & 0 & 1 & 0 \\ 0 & 0 & 1 & 0 & -1 & 0 & 0 & 0 \\ 0 & 0 & -1 & 1 & 0 & -1 & 0 & 0 \\ 0 & 0 & 0 & -1 & 0 & 0 & -1 & 0 \end{bmatrix}$$

$$\mathbf{C}_n = \text{diag}[52.50 \ 80.00 \ 52.50 \ 52.50 \ 70.00 \ 52.50] fF$$

$$\mathbf{R}_b = \text{diag}[17.5 \ 17.5 \ 17.5 \ 17.5 \ 35.0 \ 35.0 \ 35.0 \ 50.0] \Omega$$

$$\mathbf{L}_b = \text{diag}[17.53 \ 17.53 \ 17.53 \ 17.53 \ 35.07 \ 35.07 \ 35.07 \ 10.00] pH$$

For this particular case the upper-left 6×6 blocks of the first three partial sums, as well as the limit of the series are:

$$(\mathbf{B})_{n \times n} = \begin{bmatrix} 0.0291 & 0.0335 & 0.0222 & 0.0252 & 0.0314 & 0.0229 \\ 0.0220 & 0.0341 & 0.0220 & 0.0216 & 0.0289 & 0.0216 \\ 0.0222 & 0.0335 & 0.0291 & 0.0229 & 0.0314 & 0.0252 \\ 0.0252 & 0.0330 & 0.0229 & 0.0329 & 0.0370 & 0.0260 \\ 0.0236 & 0.0330 & 0.0236 & 0.0277 & 0.0401 & 0.0277 \\ 0.0229 & 0.0330 & 0.0252 & 0.0260 & 0.0370 & 0.0329 \end{bmatrix}$$

$$(\mathbf{B} + \mathbf{B}^2)_{n \times n} = \begin{bmatrix} 0.0329 & 0.0389 & 0.0261 & 0.0294 & 0.0370 & 0.0271 \\ 0.0255 & 0.0390 & 0.0255 & 0.0255 & 0.0340 & 0.0255 \\ 0.0261 & 0.0389 & 0.0329 & 0.0271 & 0.0370 & 0.0294 \\ 0.0294 & 0.0388 & 0.0271 & 0.0374 & 0.0430 & 0.0305 \\ 0.0277 & 0.0388 & 0.0277 & 0.0322 & 0.0461 & 0.0322 \\ 0.0271 & 0.0388 & 0.0294 & 0.0305 & 0.0430 & 0.0374 \end{bmatrix}$$

$$(\mathbf{B} + \mathbf{B}^2 + \mathbf{B}^3)_{n \times n} = \begin{bmatrix} 0.0336 & 0.0398 & 0.0267 & 0.0301 & 0.0379 & 0.0278 \\ 0.0261 & 0.0398 & 0.0261 & 0.0261 & 0.0348 & 0.0261 \\ 0.0267 & 0.0398 & 0.0336 & 0.0278 & 0.0379 & 0.0301 \\ 0.0301 & 0.0398 & 0.0278 & 0.0382 & 0.0440 & 0.0313 \\ 0.0284 & 0.0398 & 0.0284 & 0.0330 & 0.0471 & 0.0330 \\ 0.0278 & 0.0398 & 0.0301 & 0.0313 & 0.0440 & 0.0382 \end{bmatrix}$$

$$(\mathbf{B}(\mathbf{I} - \mathbf{B})^{-1})_{n \times n} = \begin{bmatrix} 0.0337 & 0.0400 & 0.0268 & 0.0303 & 0.0381 & 0.0280 \\ 0.0262 & 0.0400 & 0.0262 & 0.0262 & 0.0350 & 0.0262 \\ 0.0268 & 0.0400 & 0.0337 & 0.0280 & 0.0381 & 0.0303 \\ 0.0303 & 0.0400 & 0.0280 & 0.0383 & 0.0442 & 0.0314 \\ 0.0285 & 0.0400 & 0.0285 & 0.0331 & 0.0472 & 0.0331 \\ 0.0280 & 0.0400 & 0.0303 & 0.0314 & 0.0442 & 0.0383 \end{bmatrix}$$

which are all nonnegative as expected (observe the remarkably fast convergence of the series to its limit after only three partial sums).

In order, now, to prove that $\lim_{N \rightarrow \infty} \mathbf{B}^N = \mathbf{0}$ (which is necessary for the above to hold) we first establish that \mathbf{B}^N has the general form shown at the bottom of the page (just multiply \mathbf{B}^N by \mathbf{B} of (11) and verify that the resulting \mathbf{B}^{N+1} has the same form). Therefore, in order to prove that $\lim_{N \rightarrow \infty} \mathbf{B}^N = \mathbf{0}$ we just need to prove that $\lim_{N \rightarrow \infty} \mathbf{U}^N = \mathbf{0}$ and $\lim_{N \rightarrow \infty} \mathbf{Q}^N = \mathbf{0}$. For this we will need the following theorem:

Theorem 6. If $\mathbf{V} = [v_{ij}]$ is a $n \times n$ – row or column – diagonally dominant matrix with positive diagonal elements, then for the matrix $\mathbf{W} = (\mathbf{I} + \mathbf{V})^{-1}$ it holds $\lim_{N \rightarrow \infty} \mathbf{W}^N = \mathbf{0}$ (proof in Appendix A).

Since $\mathbf{Q} = (\mathbf{I}_n + \mathbf{A}_C \mathbf{U} \mathbf{A}_L)^{-1}$ where $\mathbf{A}_C \mathbf{U} \mathbf{A}_L = h \mathbf{C}_n^{-1} \mathbf{A}_{rl} \mathbf{U} h \mathbf{L}_b^{-1} \mathbf{A}_{rl}^T$ is a row diagonally dominant matrix with positive diagonal elements, the above theorem proves that $\lim_{N \rightarrow \infty} \mathbf{Q}^N = \mathbf{0}$. Also, as a special case, it proves for $\mathbf{U} = (\mathbf{I}_b + \mathbf{R}_L)^{-1}$ that $\lim_{N \rightarrow \infty} \mathbf{U}^N = \mathbf{0}$, since the positive diagonal matrix $\mathbf{R}_L = h \mathbf{L}_b^{-1} \mathbf{R}_b$ is obviously diagonally dominant with positive diagonal elements. Thus, we have finally established the nonnegativity of the upper-left blocks $(\mathbf{B})_{n \times n}$, $(\mathbf{B} + \mathbf{B}^2)_{n \times n}$, ..., $(\mathbf{B} + \mathbf{B}^2 + \dots + \mathbf{B}^N)_{n \times n}$, along with the coefficients of the linear functions $\bar{v}_i \equiv \bar{v}_i(\mathbf{y})$, $i = 1, 2, \dots, n$ in (9).

D. Extension in the case of mutual inductances

When mutual inductances are present in the model of the power grid, then the matrix \mathbf{L}_b of branch inductances is no longer positive diagonal and we cannot rigorously show that the blocks $(\mathbf{B})_{n \times n}$, $(\mathbf{B} + \mathbf{B}^2)_{n \times n}$, ..., $(\mathbf{B} + \mathbf{B}^2 + \dots + \mathbf{B}^N)_{n \times n}$ are nonnegative.

$$\mathbf{B}^N = \begin{bmatrix} \mathbf{Q}^N \pm \sum_i \left(\prod \mathbf{Q}^{N-a_i} \mathbf{A}_C \mathbf{U}^{N-b_i} \mathbf{A}_L \mathbf{Q}^{N-c_i} \right) & - \sum_j \left(\mathbf{Q}^{N-a_j} \mathbf{A}_C \mathbf{U}^{N-b_j} \right) \pm \sum_k \left(\mathbf{Q}^{N-a_k} \mathbf{A}_C \mathbf{U}^{N-a_k} \prod \mathbf{A}_L \mathbf{Q}^{N-c_k} \mathbf{A}_C \mathbf{U}^N \right) \\ \sum_l \left(\mathbf{U}^{N-a_l} \mathbf{A}_L \mathbf{Q}^{N-b_l} \right) \pm \sum_m \left(\mathbf{U}^{N-a_m} \mathbf{A}_L \mathbf{Q}^{N-b_m} \prod \mathbf{A}_C \mathbf{U}^{N-c_m} \mathbf{A}_L \mathbf{Q}^{N-d_m} \right) & \mathbf{U}^N \pm \sum_n \left(\prod \mathbf{U}^{N-a_n} \mathbf{A}_L \mathbf{Q}^{N-b_n} \mathbf{A}_C \mathbf{U}^{N-c_n} \right) \end{bmatrix}$$

However, it is known that the *inverse* \mathbf{L}_b^{-1} is a symmetric diagonally dominant matrix with positive diagonal elements [12].

With the below theorems we will prove that if \mathbf{V} is a symmetric diagonally dominant matrix with positive diagonal elements and \mathbf{D} is a positive diagonal matrix, then the matrix $(\mathbf{I} + \mathbf{VD})^{-1}\mathbf{V}$ is also symmetric diagonally dominant with positive diagonal elements.

Lemma 2. If $\mathbf{A} = [a_{ij}]$ is a $n \times n$ matrix with positive diagonal elements which satisfies $\|\mathbf{A}\|_\infty = \max_{1 \leq i \leq n} \sum_{j=1}^n |a_{ij}| < 1$ (resp., $\|\mathbf{A}\|_1 = \max_{1 \leq j \leq n} \sum_{i=1}^n |a_{ij}| < 1$), then the matrix $\mathbf{B} = \mathbf{I} - \mathbf{A}$ is row (resp., column) diagonally dominant with positive diagonal elements (proof in Appendix A).

Theorem 2. If $\mathbf{A} = [a_{ij}]$ is a $n \times n$ row diagonally dominant matrix with positive

diagonal elements then $\|\mathbf{A}^{-1}\|_\infty \leq \left[\min_{1 \leq i \leq n} \left(a_{ii} - \sum_{\substack{j=1 \\ j \neq i}}^n |a_{ij}| \right) \right]^{-1}$. If \mathbf{A} is column diagonally

dominant with positive diagonal elements then $\|\mathbf{A}^{-1}\|_1 \leq \left[\min_{1 \leq j \leq n} \left(a_{jj} - \sum_{\substack{i=1 \\ i \neq j}}^n |a_{ij}| \right) \right]^{-1}$ (proof

in Appendix A).

Theorem 3. Let $\mathbf{A} = [a_{ij}]$ be a $n \times n$ – row or column – diagonally dominant matrix with positive diagonal elements. If λ is an eigenvalue of \mathbf{A} then $\text{Re } \lambda > 0$ (proof in Appendix A).

Theorem 4. If $\mathbf{A} = [a_{ij}]$ is a $n \times n$ – row or column – diagonally dominant matrix with positive diagonal elements then \mathbf{A}^{-1} has only positive diagonal elements (proof in Appendix A).

Theorem 5. If $\mathbf{A} = [a_{ij}]$ is a $n \times n$ row (resp., column) diagonally dominant matrix with positive diagonal elements then the matrix $\mathbf{I} - (\mathbf{I} + \mathbf{A})^{-1} = (\mathbf{I} + \mathbf{A})^{-1} \mathbf{A} = (\mathbf{A}^{-1} + \mathbf{I})^{-1}$ is also row (resp., column) diagonally dominant with positive diagonal elements (proof in Appendix A).

Corollary 1. If $\mathbf{A} = [a_{ij}]$ is a $n \times n$ row (resp., column) diagonally dominant matrix with positive diagonal elements and $\mathbf{D} = [d_i]$ is a $n \times n$ positive diagonal matrix, then the matrix $(\mathbf{A}^{-1} + \mathbf{D})^{-1} = (\mathbf{I} + \mathbf{AD})^{-1} \mathbf{A}$ is also row (resp., column) diagonally dominant with positive diagonal elements (proof in Appendix A).

Thus we finally proved that if \mathbf{V} is a symmetric diagonally dominant matrix with positive diagonal elements and \mathbf{D} is a positive diagonal matrix, then the matrix $(\mathbf{I} + \mathbf{VD})^{-1} \mathbf{V}$ is also symmetric diagonally dominant with positive diagonal elements. This result applies to the matrix $\mathbf{U}h\mathbf{L}_b^{-1} = (\mathbf{I}_b + h\mathbf{L}_b^{-1}\mathbf{R}_b)^{-1}h\mathbf{L}_b^{-1}$ which is hence symmetric diagonally dominant with positive diagonal elements. Due to its diagonal dominance property, the matrix $\mathbf{U}h\mathbf{L}_b^{-1}$ (especially if it is a large one) is expected to behave a lot like a positive diagonal matrix within the product $\mathbf{A}_{rl}(\mathbf{U}h\mathbf{L}_b^{-1})\mathbf{A}_{rl}^T$ and produce a matrix where the entries originating from diagonal elements “dominate”. Therefore the results of the previous section derived for a positive diagonal \mathbf{L}_b^{-1} are expected to still hold because \mathbf{L}_b^{-1} is now diagonally dominant with positive diagonal elements. In particular, the matrix $\mathbf{I}_n + \mathbf{A}_c \mathbf{U} \mathbf{A}_L = \mathbf{I}_n + h\mathbf{C}_n^{-1} \mathbf{A}_{rl} \mathbf{U} h\mathbf{L}_b^{-1} \mathbf{A}_{rl}^T$ is expected to be an M-matrix or quite like an M-matrix and still be inverse-nonnegative, i.e. $\mathbf{Q} = (\mathbf{B})_{n \times n} \geq 0$.

To demonstrate with a practical example, consider the same grid as in the previous section, but with the following branch inductance matrix which also has mutual inductances between branches (this matrix is an expansion of the matrix given in [12]):

$$\mathbf{L}_b = \begin{bmatrix} 11.4 & 4.2 & 2.5 & 1.8 & 1.4 & 1.1 & 0.9 & 0.7 \\ 4.2 & 11.4 & 4.2 & 2.5 & 1.8 & 1.4 & 1.1 & 0.9 \\ 2.5 & 4.2 & 11.4 & 4.2 & 2.5 & 1.8 & 1.4 & 1.1 \\ 1.8 & 2.5 & 4.2 & 11.4 & 4.2 & 2.5 & 1.8 & 1.4 \\ 1.4 & 1.8 & 2.5 & 4.2 & 11.4 & 4.2 & 2.5 & 1.8 \\ 1.1 & 1.4 & 1.8 & 2.5 & 4.2 & 11.4 & 4.2 & 2.5 \\ 0.9 & 1.1 & 1.4 & 1.8 & 2.5 & 4.2 & 11.4 & 4.2 \\ 0.7 & 0.9 & 1.1 & 1.4 & 1.8 & 2.5 & 4.2 & 11.4 \end{bmatrix} pH$$

The inverse of \mathbf{L}_b is easy to verify that it is symmetric diagonally dominant with positive diagonal elements. The matrix $\mathbf{I}_n + \mathbf{A}_C \mathbf{U} \mathbf{A}_L$ is then the following:

$$\begin{bmatrix} 163.30 & -108.47 & 0.24 & -54.43 & 0.08 & 0.30 \\ -71.18 & 203.84 & -71.13 & -0.05 & -35.57 & 0.07 \\ 0.24 & -108.39 & 163.45 & 0.19 & -0.09 & -54.37 \\ -54.43 & -0.07 & 0.19 & 163.53 & -108.35 & 0.13 \\ 0.06 & -40.66 & -0.07 & -81.26 & 204.31 & -81.39 \\ 0.30 & 0.11 & -54.37 & 0.13 & -108.52 & 163.27 \end{bmatrix}$$

Observe that the entries not originating from diagonal elements are over two orders of magnitude smaller than those originating from diagonal elements, and normally do not play any role in the matrix properties. Indeed, this matrix is inverse-nonnegative, as can be easily verified.

For the sake of comparison, consider the same branch inductance matrix but without mutual inductances, i.e. the diagonal matrix:

$$\mathbf{L}_b = \text{diag}[11.4 \ 11.4 \ 11.4 \ 11.4 \ 11.4 \ 11.4 \ 11.4 \ 11.4] pH$$

The matrix $\mathbf{I}_n + \mathbf{A}_C \mathbf{U} \mathbf{A}_L$ becomes now:

$$\begin{bmatrix} 163.38 & -108.13 & 0 & -54.24 & 0 & 0 \\ -70.96 & 203.47 & -70.96 & 0 & -35.59 & 0 \\ 0 & -108.13 & 163.38 & 0 & 0 & -54.24 \\ -54.24 & 0 & 0 & 163.38 & -108.13 & 0 \\ 0 & -40.68 & 0 & -81.10 & 203.89 & -81.10 \\ 0 & 0 & -54.24 & 0 & -108.13 & 163.38 \end{bmatrix}$$

which is a proper M-matrix.

For the same reason as above it is expected that $\lim_{N \rightarrow \infty} \mathbf{Q}^N = \mathbf{0}$. That also $\lim_{N \rightarrow \infty} \mathbf{U}^N = \mathbf{0}$ can be proved directly from Theorem 6 and the fact that $\mathbf{R}_L = h\mathbf{L}_b^{-1}\mathbf{R}_b$ is now column diagonally dominant with positive diagonal elements (on account of Lemma 1). Therefore the series $\mathbf{B} + \mathbf{B}^2 + \dots$ is still expected to converge to the limit (12), whose upper-left $n \times n$ block, given by (13), is independent of \mathbf{L}_b and is always nonnegative. This establishes the nonnegativity of the upper-left $n \times n$ blocks of all intermediate partial sums $\mathbf{B} + \mathbf{B}^2, \mathbf{B} + \mathbf{B}^2 + \mathbf{B}^3, \dots$.

Before closing this section, we remark that the nonnegative coefficients of $\bar{\mathbf{v}}_n$ in (7) also establish that the mean – or the integral of – voltage drop within a time interval is *monotone* on the vector of excitations (meaning that increasing the current at any sink and at any time instant can only result in the increase of the mean voltage drop) which has long been known for R or RC grid models [14] but was an open problem for general RLC models (and, in fact, it does *not* hold for the instantaneous value of voltage drop).

V. DEVELOPMENT OF A PRACTICAL POWER GRID VERIFICATION METHODOLOGY

There can possibly be a variety of ways to estimate the maximal subset of the excitation space of a digital circuit in order to employ it for verification of the power grid. In this paper, like in [15], we have adopted a statistical estimation framework, which consists of acquiring a sample of discretized current waveforms drawn from the sinks for a number of binary input vectors, computing the sample's own set of maximal points, and then statistically projecting this set to the expected global position of the maximal subset of the excitation space.

To be more specific, we first acquire a sample $S = \{\mathbf{y}_1, \mathbf{y}_2, \dots, \mathbf{y}_l\}$ of mN -dimensional waveform super-vectors (henceforth referred to as the “sample space”) by simulating the digital circuit for l random binary vector pairs $\{\mathbf{b}_p, \mathbf{b}_n\}$. This multivariate sample is made up of an assortment of mN univariate samples $S_i = \{y_{i,1}, y_{i,2}, \dots, y_{i,l}\}$, $i = 1, 2, \dots, mN$, each one representing the current observed at one sink and at a particular time instant for the l random vector pairs $\{\mathbf{b}_p, \mathbf{b}_n\}$. In each univariate sample S_i we can estimate the expected maximum $\omega(y_i)$ of the random variable y_i sampled by S_i by results from statistical extreme value theory. Specifically, if S_i is partitioned into l/r sub-samples of size r from which the maxima units $z_{i,j} = \max\{y_{i,(j-1)r+1}, \dots, y_{i,jr}\}$, $j = 1, 2, \dots, l/r$, are taken out to create a new sample $Z_i = \{z_{i,1}, z_{i,2}, \dots, z_{i,l/r}\}$ of size l/r , then an estimate for the expected maximum $\omega(y_i)$ of y_i can be computed as follows [13]:

$$(14) \quad \hat{\omega}(y_i) = \hat{\mu}_i + \frac{\hat{\sigma}_i}{1 + r\sqrt{\pi \log r}(\operatorname{erf}(\sqrt{\log r}) - 1)}$$

where $\operatorname{erf}(x) = \frac{2}{\sqrt{\pi}} \int_0^x \exp(-t^2) dt$ is the “error function” and $\hat{\mu}_i, \hat{\sigma}_i$ are estimates of the location-scale parameters of the asymptotic extreme value distribution (not related to the corresponding parameters of the normal distribution), which are usually

obtained by Maximum Likelihood (ML) estimation on the sample Z_i . However, due to the large dimension (mN) of the space of current waveforms it is somewhat impractical (though not entirely prohibitive) to perform ML estimation (meaning the solution of a nonlinear optimization program) for all $i=1,2,\dots,mN$, and we have instead used the method of matching the first and second moments (i.e. mean and standard deviation) of the sample Z_i with those of the extreme value distribution, by which we have [13]:

$$(15a) \quad \hat{\sigma}_i = (\sqrt{6} / \pi) \text{std}(Z_i)$$

$$(15b) \quad \hat{\mu}_i = \text{mean}(Z_i) - \gamma \hat{\sigma}_i$$

where $\gamma \approx 0.5772\dots$ is the “Euler gamma” constant. Experiments have shown that the above approximations found by moment matching are remarkably close to the actual ML estimates.

Now, the sample space $S = \{\mathbf{y}_1, \mathbf{y}_2, \dots, \mathbf{y}_l\}$ has a set of maximal points of its own, which will be scaled *down* in each individual coordinate $i=1,2,\dots,mN$ (Fig. 4) with respect to the maximal subset of the excitation space D (since there will always be points $\mathbf{y} \in D$ lying outside the outermost boundary of S). A reasonable approximation for this down-scaling of the maximal subset as a *whole* in each $i=1,2,\dots,mN$ is $\omega(y_i) - \max\{y_{i,1}, y_{i,2}, \dots, y_{i,l}\}$, where $\max\{y_{i,1}, y_{i,2}, \dots, y_{i,l}\}$ is the maximum value of each univariate sample S_i (i.e. the maximum of the sample space S in each coordinate axis). Writing this succinctly in vector form for all $i=1,2,\dots,mN$ as:

$$(16) \quad \mathbf{d} \equiv \boldsymbol{\omega}(\mathbf{y}) - \max\{\mathbf{y}_1, \mathbf{y}_2, \dots, \mathbf{y}_l\}$$

(where the max operator is interpreted component-wise) we have a difference vector by which we can shift the maximal subset of S in order to move it to the expected location of the maximal subset of D in \mathcal{R}^{mN} . It must, of course, be mentioned that the maximal subset of D will have much different structure and include many more points than the maximal subset of S , but the maximum value of a linear function is fairly

insensitive to the local structure of the maximal subset and instead depends predominantly on its global position in \Re^{mN} (Fig. 5). In order, finally, to compute the maximal points of the space S consisting of l points, we have to compare each point to all others (to determine whether a specific point is *not* dominated by *any* others in *all* components, according to Definition 1), which leads to a total of l^2 comparisons. It can be shown [14], however, that the necessary comparisons can be reduced to at most $O(l(\log_2 l)^{mN-2})$, where mN is the dimension of the space and its constituent points.

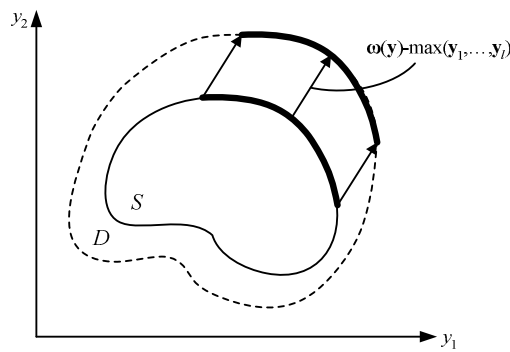


Fig. 4. Sample space S and shift of its maximal points towards the expected position of the maximal points of the excitation space D .

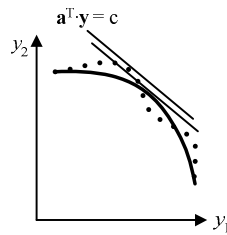


Fig. 5. Insensitivity of the maximum of a linear function to the local structure of the subset of maximal points.

VI. FLOW OF THE ALGORITHM AND COMPLEXITY ANALYSIS

For each digital circuit the process of creation of the sample space S (by circuit simulation), univariate extreme value estimation in each of the coordinate axes $i = 1, 2, \dots, mN$, and shifting of the maximal points of S (towards the global position of the maximal points of the excitation space) is *independent* of the supplying power grid and needs to be carried out only once. The main steps in this process are summarized hereafter along with some brief remarks on their implementation and computational complexity:

- *Generate a total of $l = 2500$ random pairs of binary vectors $\{\mathbf{b}_p, \mathbf{b}_n\}$ for the circuit under consideration.* This step can be performed by any standard random number generator producing uniform numbers. The selection $l = 2500$ for the number of input pairs is discussed below.
- *Simulate the circuit under all generated pairs and record the discretized current waveforms in each sink $j = 1, 2, \dots, m$ and for each time instant $t = kh$, $k = 1, 2, \dots, N$ within an interval of interest (e.g. a clock period).* The recorded data $S_i = \{y_{i,1}, y_{i,2}, \dots, y_{i,l}\}$, $i = 1, 2, \dots, mN$, taken jointly as mN -dimensional vectors will constitute the sample space $S = \{\mathbf{y}_1, \mathbf{y}_2, \dots, \mathbf{y}_l\}$. The number N of time instants within an interval can be kept small, as seen in the examples of the previous section (a number $N = 10$ should be enough). The computational time required to complete this step is entirely up to the simulator program employed, since there are many different simulators with speeds that range considerably depending on the detail of the analysis and their algorithmic efficiency. Although larger circuits will definitely take longer to simulate for every clock cycle, we must emphasize that a total of 2500 binary input pairs is sufficient to produce a reasonable statistical estimate *independently* of the circuit size or sink size, as is further explained below.

- Arrange each univariate sample S_i , $i = 1, 2, \dots, mN$, into $l/r = 100$ sub-samples of size $r = 25$. Here the size r only needs to be adequate so that the sample of the maxima units from the sub-samples follows an asymptotic extreme value distribution. We have found by experimentation that $r = 25$ is a fair value. The number $l/r = 100$ of sub-samples (leading to a total of $l = 2500$ units) yields estimates with relative estimation error (i.e. quotient of confidence interval to estimate) of about 5% – at a confidence level 95% – for *any* sink irrespective of its size or the size of the broader circuit, as was observed in [13]. This happens because with an increase in the sink size, both the mean and the standard deviation of the distribution of sink currents are increased, but their ratio which determines the relative estimation error remains roughly constant. Only in the case where a smaller estimation error and/or a higher confidence level are desired, the number l/r of sub-samples will have to be increased (together with the total number l of input pairs).
- For each $i = 1, 2, \dots, mN$ construct the sample Z_i of the maxima units from the l/r sub-samples of S_i .
- For each $i = 1, 2, \dots, mN$ calculate the estimates $\hat{\mu}_i, \hat{\sigma}_i$ of the extreme value distribution parameters from (15), and the estimate $\hat{\omega}(y_i)$ of the expected maximum $\omega(y_i)$ from (14).
- Determine the maxima $\max\{y_{i,1}, y_{i,2}, \dots, y_{i,l}\}$ of all univariate samples S_i , $i = 1, 2, \dots, mN$, and in conjunction with the estimates $\hat{\omega}(y_i)$, $i = 1, 2, \dots, mN$ for the expected maxima, compute the mN -dimensional difference vector \mathbf{d} from (16).
- Locate the maximal points of the sample space S . As already mentioned, this step has complexity of $O(l(\log_2 l)^{mN-2})$ comparisons.
- Shift the maximal points of the sample space S by the computed difference vector \mathbf{d} . This step is performed by plain component-wise addition of the vector \mathbf{d} to the maximal points of S , and is a trivial one.

The output of all the above steps is a set of shifted sample maximal points for a particular circuit which approximate the position of the maximal points of its excitation space, and thus constitute worst-case waveform excitations for any grid supplying the circuit.

Having extracted a set of worst-case current waveforms, the verification of any given grid can be performed as follows:

- *Apply the shifted maximal points as excitation waveforms in a linear network simulator to perform an analogous number of transient analyses for the given power grid.* This step relies exclusively on a linear network simulator, and its execution time is determined by the capability of the simulator to carry out the required analyses for the given grid.
- *For each sink $j = 1, 2, \dots, m$ compute the mean voltage drop for each transient analysis and determine the maximum value among the computed mean voltage drops.* The resulting value for each sink finally constitutes an estimate of the worst-case cycle-mean voltage drop over all possible cycles and corresponding binary vector pairs.

On the basis of the same set of worst-case current waveforms the solution of optimization problem (1) (minimizing grid area subject to voltage drop at all active modules, wire widths and decoupling capacitor lengths) and optimization problem (2) (minimizing grid noise subject to wire widths and decoupling capacitor lengths) consist of three main stages:

- 1) Evaluation of objective function and constraints at the current value of the parameter vector. The evaluation of the voltage drop constraints in problem (1) or the noise metric (objective function) in problem (2) is performed by transient analysis of the power grid.

- 2) Calculate the sensitivities (or gradient vector) of the parameters at the current step. These can be calculated either by finite difference approximations or by the method of adjoint networks [16].
- 3) Update vector of parameters according to their sensitivities. The procedure solves a quadratic subproblem in each iteration step, resulting from a quadratic approximation of the Lagrangian function [17]-[18].

VII. EXPERIMENTAL RESULTS

In order to validate our method we have generated a number of test power grids (since there are no universally accepted benchmarks) that will be denoted as $Gn-p$, where n stands for the number of all (internal/sink/voltage) nodes and p for the number of voltage nodes on which supply pads are to be connected (e.g. the label G150-6 denotes a grid with 150 nodes and 6 supply pads). All test grids were uniform rectangular meshes and had equal widths for all branches in every straight line (horizontal or vertical). For the digital circuits supplied by the grids we have implemented the traditional ISCAS85 benchmarks in $0.09\mu m$ technology, and partitioned each one of them to a number of functional modules (representing the m current sinks). The placements of the current sinks and the power pads across the grid area were chosen in random. Decoupling capacitors were placed in every node of the grid.

The results for the maximum voltage drops in various test grids supplying some of the ISCAS85 benchmark circuits are shown in Table I. All computed worst-case voltage drops are compared to accurate statistical estimates obtained by directly applying the univariate extreme value estimation procedure (relations (14) and (15)) on samples of voltage drops for the same $l = 2500$ input pairs (it must be stressed, however, that a direct statistical estimation of maximum voltage drop – instead of determining the worst-case current excitations – is not a viable solution for power grid verification, since the grid typically undergoes many iterations of redesign and verification with the same underlying circuit until deemed robust). From the table it can be readily verified that the two estimates come remarkably close to each other. A slight pessimism which is observed for the proposed method is not a matter of concern (since it will not lead to any grid underdesign), and can possibly be attributed to the deviation of the shifted maximal points of the sample space compared to the maximal points of the excitation space which eventually seems to lie on the pessimistic side (i.e. the vector (16) slightly overestimates their relative positions).

Table I. Maximum voltage drop (accurate and pessimistic results) at two current sinks for various benchmark circuits and test power grids.

Case study	Grid	Circuit	Max. voltage drop to sink-A (mV)				Max. voltage drop to sink-B (mV)			
			Our Method	Statistical estimation	Pessimistic analysis (MEC)	% difference	Our method	Statistical estimation	Pessimistic analysis (MEC)	% difference
#1	G25-2	c1355	539.2	481.5(±40.5)	732.5	35.9	548.5	494.0(±41.7)	743.8	35.6
#2	G50-3	c1355	303.7	275.6(±23.9)	416.7	37.2	292.1	265.2(±23.1)	397.8	36.2
#3	G75-6	c1355	141.7	129.6(±11.5)	190.1	34.1	126.	115.5(±10.3)	168.8	33.9
#4	G100-10	c1355	57.1	52.2(±4.7)	77.8	36.2	54.1	49.4(±4.4)	73.7	36.1
#5	G150-10	c1355	56.6	51.7(±4.6)	77.1	36.1	55.5	50.6 (±4.5)	75.5	36.0
#6	G150-15	c1355	72.2	65.0(±5.4)	98.2	36.0	71.1	65.9(±5.6)	96.5	35.8
#7	G100-6	c2670	230.8	167.7(±11.4)	341.5	48.0	224.7	163.7(±11.1)	332.4	47.9
#8	G150-10	c2670	119.4	90.4(±6.6)	178.7	49.6	119.5	93.0(±6.8)	178.6	49.4
#9	G150-15	c2670	87.3	65.4(±4.6)	134.1	53.5	69.6	52.3(±3.7)	106.4	52.8
#10	G225-10	c2670	185.7	138.6(±9.4)	275.9	48.5	185.9	140.1(±9.8)	274.1	47.4
#11	G400-10	c2670	82.9	63.3(±4.6)	126.1	52.1	81.5	61.6(±4.5)	122.2	49.9
#12	G625-15	c2670	66.6	49.5 (±3.4)	98.6	48.0	65.0	48.6(±3.4)	96.0	47.8
#13	G400-10	c6288	160.7	121.1(±3.7)	247.2	53.8	157.6	118.7(±3.7)	242.0	53.6
#14	G400-15	c6288	108.0	80.3(±2.1)	166.5	54.1	112.0	83.2(±2.3)	172.5	54.0
#15	G900-15	c6288	107.5	81.8(±2.7)	165.7	54.2	104.7	79.8(±2.5)	161.4	54.1
#16	G1369-20	c6288	69.0	52.2(±1.6)	106.0	53.5	67.9	51.4(±1.5)	104.3	53.5
#17	G400-10	c7552	425.7	343.7(±30.4)	590.8	38.8	433.4	350.1(±31.0)	601.1	38.7
#18	G400-15	c7552	248.9	200.2(±17.9)	345.0	38.6	229.3	184.5(±16.4)	317.7	38.5
#19	G900-15	c7552	290.7	232.4(±20.5)	400.8	37.9	299.3	239.4(±21.1)	412.4	37.8
#20	G1369-20	c7552	191.9	153.1(±13.5)	265.6	38.4	194.3	154.9(±13.7)	268.5	38.2

For every case a pessimistic analysis has also been carried out by forming a fictitious waveform consisting of the estimates of the expected maxima $\hat{\omega}(y_i)$, $i = 1, 2, \dots, mN$, for each sink and each time instant. This is effectively a construction of the Maximum Envelope Current (MEC) waveform that was introduced in [19] and which was subsequently used in a number of papers as a (pessimistic) upper bound waveform for power grid verification. We can clearly see the overestimation incurred by this pessimistic analysis which is above 30% even for a small circuit such as the c1355, and reaches 55% for c6288 which is one of the largest circuits among the tested benchmarks. Since the ISCAS85 benchmarks are actually small circuits compared to today's standards, the differences between the proposed method and the MEC-based analysis are expected to be a lot more pronounced in the case of larger designs with several current sinks and more complex interdependencies between them.

Timing analysis for the above simulations is shown in Table II. In the fourth column one can see the number of maximal points. In the fifth column there is the time for statistical maximal estimation and calculation of differential vector (statistical estimation). In the next column there is time for calculation and shifting of maximal points (shift maximal points). The next four columns show time for system matrix decomposition (T1), time for estimation with maximal excitations (T2), time for direct statistical estimation (T3) and time for estimation with MEC excitations (T4).

Table I. Timing Analysis

Case study	Grid	Circuit	#maximal points	Statistical estimation (sec)	Shift Maximal Points (sec)	T1 (sec)	T2 (sec)	T3 (sec)	T4 (sec)
#1	G25-2	c1355	1547	0	2.184	0	0.499	0.827	0
#2	G50-3	c1355	1430	0	2.074	0	1.857	3.291	0
#3	G75-6	c1355	1479	0	2.356	0.016	4.758	7.925	0
#4	G100-10	c1355	1434	0.002	2.133	0.044	8.144	14.042	0.005
#5	G150-10	c1355	1434	0.002	2.216	0.107	17.777	31.15	0.013
#6	G150-15	c1355	1547	0.003	2.237	0.086	17.979	31.351	0.013
#7	G100-6	c2670	2440	0.006	8.638	0.033	13.105	13.456	0.005
#8	G150-10	c2670	2427	0.007	8.573	0.141	33.066	32.084	0.013
#9	G150-15	c2670	2434	0.008	8.721	0.067	30.888	31.937	0.013
#10	G225-10	c2670	2431	0.006	8.441	0.294	68.193	70.515	0.028
#11	G400-10	c2670	2434	0.007	8.639	1.172	267.478	263.862	0.105
#12	G625-15	c2670	2417	0.006	8.592	4.522	687.2	715.483	0.289
#13	G400-10	c6288	2500	0.017	21.064	1.228	260.711	261.976	0.106
#14	G400-15	c6288	2500	0.016	21.014	1.17	274.563	273.139	0.11
#15	G900-15	c6288	2500	0.047	20.701	13.104	1660.839	1659.186	0.586
#16	G1369-20	c6288	2500	0.018	20.768	46.116	3649.444	3611.215	1.407
#17	G400-10	c7552	2200	0.031	25.581	1.235	231.737	263.046	0.105
#18	G400-15	c7552	2262	0.031	25.772	1.155	230.709	256.074	0.109
#19	G900-15	c7552	2258	0.026	26.22	13.315	1443.437	1663.997	0.735
#20	G1369-20	c7552	2262	0.022	25.493	45.975	3212.779	3674.132	1.416

The results for area optimization are shown in Table III. In the second column there is the power grid and in the third column there is the circuit that is being optimized. The power grid wire area and the decoupling capacitor area are shown in the next two columns (Wire area and Decap area). Total area is shown in column six (Total area) while pessimistic total area is shown in column seven (Pessimistic total area). Perc is the percentage difference of the (value of the) objective function between our method and the pessimistic analysis and is shown in the last column.

Table III . Area Optimization

Case Study	Grid	Circuit	Wire Area (m)	Decap Area (m)	Total area (m)	Pessimistic Total Area (m)	Perc%
#1	G100-6	C1355	3.2529e-9	2.4305e-8	2.7558e-8	3.1879e-8	15.7
#2	G100-10	C1355	4.0187e-9	2.3340e-8	2.7359e-8	2.9639e-8	8.3
#3	G150-10	C1355	4.1355e-9	2.2007e-8	2.6143e-8	3.3370e-8	27.7
#4	G150-15	C1355	5.1579e-9	1.9424e-8	2.4582e-8	2.9115e-8	18.4
#5	G100-6	C2670	3.1609e-9	3.5151e-8	3.8312e-8	4.6509e-8	21.4
#6	G100-10	C2670	3.1898e-9	3.2006e-8	3.5196e-8	4.4554e-8	26.6
#7	G150-10	C2670	4.3022e-9	3.3103e-8	3.7405e-8	4.4685e-8	19.5
#8	G150-15	C2670	3.8773e-9	2.7992e-8	3.1869e-8	4.1320e-8	29.7

In some first experiments we placed decoupling capacitors only in voltage and current nodes, since grid noise is higher in these nodes.

We set as an initial starting point for wire width $1\mu m$ and as an initial starting point for decoupling capacitor length $250\mu m$, as decoupling capacitors are expected to occupy bigger area.

The wire widths are assumed to be $0.4\mu m$ as a lower bound and as an upper bound was used the vertical size of the chip for vertical wires and the horizontal size of the chip for horizontal wires.

We set the lower bound for the length of decoupling capacitors as $0.4\mu m$ because it is a small value that does not affect the overall optimization and is not zero, since we wanted every node to have a decoupling capacitor.

We set the upper bound for the length of decoupling capacitors as the horizontal size of the chip but such a size for a decoupling capacitor was not enough to deteriorate the voltage drop effect, especially for circuits with a small number of voltage nodes. Hence, we added decoupling capacitors in every node of the grid and set a higher value for an upper bound of a decoupling capacitor length. This slightly perturbed simulation time and resulted in more reasonable lengths for decoupling capacitors.

The wire widths as well as the decoupling capacitors lengths returned by the optimizer are continuously between the lower and the upper bound. The wire widths are usually near the lower bound. Decoupling capacitors placed in nodes where current sinks are placed tend to be bigger (this happens in order to deteriorate grid noise).

The results for noise optimization are shown in Table IV. In the second and third column one can see the power grid and the circuit being optimized. Voltage Drop is the value of the objective function for our method, which is actually the sum of voltage drop at nodes where the noise-metric is above the threshold, and is shown in the next column. Pessimistic Voltage Drop which is shown in fifth column is the value of the objective function for the pessimistic analysis. Perc is the percentage difference of the (value of the) objective function between our method and the pessimistic analysis and is shown in the last column.

Table IV. Noise Optimization

Case Study	Grid	Circuit	Voltage drop (V)	Pessimistic Voltage Drop (V)	Perc%
#1	G100-6	C1355	84.6	110.3	30.4
#2	G100-10	C1355	62.1	82.9	33.5
#3	G150-10	C1355	54.7	77.3	41.2
#4	G150-15	C1355	42.6	59.7	40.1
#5	G100-6	C2670	142.5	199.8	40.2
#6	G100-10	C2670	111.6	159.6	43.0
#7	G150-10	C2670	115.3	171.0	48.2
#8	G150-15	C2670	83.8	131.0	56.2
#9	G400-10	C7552	825.2	1038.7	25.9
#10	G400-15	C7552	746.1	944.9	26.6

We can see that when simulating a circuit with the same grid and different amount of voltage nodes we get lower voltage drop for the circuit which has more voltage nodes. Wire widths and decoupling capacitor lengths reach the upper bounds for almost all cases.

We can see that in noise optimization problem we get even better results for the percentage difference between our method and the pessimistic analysis, even for larger circuits.

APPENDIX A

PROOFS OF THE ALGORITHMS

Lemma 1. If $\mathbf{V} = [v_{ij}]$ is a $n \times n$ symmetric diagonally dominant matrix with positive diagonal elements and nonpositive off-diagonal elements, and $\mathbf{C} = [c_i]$, $\mathbf{D} = [d_i]$ are $n \times n$ positive and nonnegative diagonal matrices respectively (i.e. $c_i > 0$ and $d_i \geq 0$, $i = 1, \dots, n$), then $\mathbf{W} = \mathbf{D} + \mathbf{CV}$ is a $n \times n$ row diagonally dominant matrix and $\mathbf{Y} = \mathbf{D} + \mathbf{VC}$ is a $n \times n$ column diagonally dominant matrix, both with positive diagonal elements and nonpositive off-diagonal elements.

Proof. It is easily observed that the ij th element of the matrix product \mathbf{CV} equals $c_i v_{ij}$ (i.e. the effect of pre-multiplying a matrix \mathbf{V} by a diagonal matrix \mathbf{C} is simply to multiply each element of the i th row of \mathbf{V} by the i th diagonal element of \mathbf{C}). Similarly, the ij th element of \mathbf{VC} equals $c_j v_{ij}$ (i.e. the effect of post-multiplying a matrix \mathbf{V} by a diagonal matrix \mathbf{C} is to multiply each element of the j th column of \mathbf{V} by the j th diagonal element of \mathbf{C}). Then for the matrix \mathbf{W} we have $w_{ii} = d_i + c_i v_{ii} > 0$ ($i = 1, \dots, n$) and $w_{ij} = c_i v_{ij} \leq 0$ ($i, j = 1, \dots, n$, $i \neq j$), and also:

$$w_{ii} = d_i + c_i v_{ii} \geq d_i + c_i \sum_{\substack{j=1 \\ j \neq i}}^n |v_{ij}| \geq \sum_{\substack{j=1 \\ j \neq i}}^n |c_i v_{ij}| = \sum_{\substack{j=1 \\ j \neq i}}^n |w_{ij}|, \quad \forall i = 1, \dots, n$$

i.e. \mathbf{W} is a row diagonally dominant matrix.

Likewise, for \mathbf{Y} we have $y_{jj} = d_j + c_j v_{jj} > 0$ ($j = 1, \dots, n$) and $y_{ij} = c_j v_{ij} \leq 0$ ($i, j = 1, \dots, n$, $i \neq j$), and also:

$$y_{jj} = d_j + c_j v_{jj} \geq d_j + c_j \sum_{\substack{i=1 \\ i \neq j}}^n |v_{ij}| \geq \sum_{\substack{i=1 \\ i \neq j}}^n |c_j v_{ij}| = \sum_{\substack{i=1 \\ i \neq j}}^n |y_{ij}|, \quad \forall j = 1, \dots, n$$

i.e. \mathbf{Y} is a column diagonally dominant matrix. **Q.E.D.**

Lemma 2. If $\mathbf{A} = [a_{ij}]$ is a $n \times n$ matrix with positive diagonal elements which satisfies $\|\mathbf{A}\|_{\infty} = \max_{1 \leq i \leq n} \sum_{j=1}^n |a_{ij}| < 1$ (resp., $\|\mathbf{A}\|_1 = \max_{1 \leq j \leq n} \sum_{i=1}^n |a_{ij}| < 1$), then the matrix $\mathbf{B} = \mathbf{I} - \mathbf{A}$ is row (resp., column) diagonally dominant with positive diagonal elements.

Proof. If $\|\mathbf{A}\|_{\infty} = \max_{1 \leq i \leq n} \sum_{j=1}^n |a_{ij}| < 1$, then $\sum_{j=1}^n |a_{ij}| < 1, \forall i = 1, \dots, n$, or (considering also that $a_{ii} > 0, i = 1, \dots, n$):

$$0 < \sum_{\substack{j=1 \\ j \neq i}}^n |a_{ij}| = \sum_{\substack{j=1 \\ j \neq i}}^n |b_{ij}| < 1 - a_{ii} = b_{ii}, \forall i = 1, \dots, n$$

i.e. $\mathbf{B} = \mathbf{I} - \mathbf{A}$ is row diagonally dominant with positive diagonal elements.

Likewise, if $\|\mathbf{A}\|_1 = \max_{1 \leq j \leq n} \sum_{i=1}^n |a_{ij}| < 1$, then $\sum_{i=1}^n |a_{ij}| < 1, \forall j = 1, \dots, n$, or (considering also that $a_{jj} > 0, j = 1, \dots, n$):

$$0 < \sum_{\substack{i=1 \\ i \neq j}}^n |a_{ij}| = \sum_{\substack{i=1 \\ i \neq j}}^n |b_{ij}| < 1 - a_{jj} = b_{jj}, \forall j = 1, \dots, n$$

i.e. $\mathbf{B} = \mathbf{I} - \mathbf{A}$ is column diagonally dominant with positive diagonal elements.
Q.E.D.

Theorem 1. [15] Let $f(\mathbf{y}) = \sum_{i=1}^M a_i y_i = \mathbf{a}^T \cdot \mathbf{y}$ be a linear (or linear affine) function with nonnegative coefficient vector \mathbf{a} (i.e. $\mathbf{a} \geq \mathbf{0}$ component-wise) which is defined on a compact set $D \subset \mathbb{R}^M$. If $\mathbf{y}^* \in D$ is a maximizer of $f(\mathbf{y})$ [i.e. $f(\mathbf{y}^*) = \max_{\mathbf{y} \in D} f(\mathbf{y})$], then \mathbf{y}^* is a maximal point of D .

Theorem 2. If $\mathbf{A} = [a_{ij}]$ is a $n \times n$ row diagonally dominant matrix with positive

diagonal elements then $\|\mathbf{A}^{-1}\|_{\infty} \leq \left[\min_{1 \leq i \leq n} \left(a_{ii} - \sum_{\substack{j=1 \\ j \neq i}}^n |a_{ij}| \right) \right]^{-1}$. If \mathbf{A} is column diagonally

dominant with positive diagonal elements then $\|\mathbf{A}^{-1}\|_1 \leq \left[\min_{1 \leq j \leq n} \left(a_{jj} - \sum_{\substack{i=1 \\ i \neq j}}^n |a_{ij}| \right) \right]^{-1}$.

Proof. For every induced matrix norm it is:

$$\|\mathbf{A}^{-1}\| = \sup_{\substack{\mathbf{x} \in \mathfrak{R}^n \\ \mathbf{x} \neq \mathbf{0}}} \frac{\|\mathbf{A}^{-1}\mathbf{x}\|}{\|\mathbf{x}\|} = \sup_{\substack{\mathbf{x} \in \mathfrak{R}^n \\ \mathbf{x} \neq \mathbf{0}}} \frac{\|\mathbf{A}^{-1}\mathbf{x}\|}{\|\mathbf{A}\mathbf{A}^{-1}\mathbf{x}\|} = \sup_{\substack{\mathbf{y} \in \mathfrak{R}^n \\ \mathbf{y} \neq \mathbf{0}}} \frac{\|\mathbf{y}\|}{\|\mathbf{A}\mathbf{y}\|} = \left[\inf_{\substack{\mathbf{y} \in \mathfrak{R}^n \\ \mathbf{y} \neq \mathbf{0}}} \frac{\|\mathbf{A}\mathbf{y}\|}{\|\mathbf{y}\|} \right]^{-1}$$

(provided, of course, that \mathbf{A} is nonsingular). Now, if \mathbf{A} is row diagonally dominant with positive diagonal elements (in which case \mathbf{A}^{-1} always exists [23]), then in order

to show that $\|\mathbf{A}^{-1}\|_{\infty} \leq \left[\min_{1 \leq i \leq n} \left(a_{ii} - \sum_{\substack{j=1 \\ j \neq i}}^n |a_{ij}| \right) \right]^{-1}$ we just need to show that

$$\frac{\|\mathbf{A}\mathbf{y}\|_{\infty}}{\|\mathbf{y}\|_{\infty}} \geq \min_{1 \leq i \leq n} \left(a_{ii} - \sum_{\substack{j=1 \\ j \neq i}}^n |a_{ij}| \right) > 0, \quad \forall \mathbf{y} \in \mathfrak{R}^n. \text{ Assume that for some arbitrary vector}$$

$\mathbf{y} \in \mathfrak{R}^n$ it is $|y_k| = \|\mathbf{y}\|_{\infty} = \max_{1 \leq i \leq n} |y_i|$. Then we have:

$$\frac{\|\mathbf{A}\mathbf{y}\|_{\infty}}{\|\mathbf{y}\|_{\infty}} = \frac{\max_{1 \leq i \leq n} \left| \sum_{j=1}^n a_{ij} y_j \right|}{|y_k|} \geq \frac{\left| \sum_{j=1}^n a_{kj} y_j \right|}{|y_k|} \geq \frac{\left| a_{kk} y_k - \sum_{\substack{j=1 \\ j \neq k}}^n a_{kj} y_j \right|}{|y_k|} \geq \frac{\left| a_{kk} y_k \right| - \sum_{\substack{j=1 \\ j \neq k}}^n |a_{kj}| |y_j|}{|y_k|}$$

$$\geq \frac{\left| a_{kk} y_k \right| - \sum_{\substack{j=1 \\ j \neq k}}^n |a_{kj}| |y_k|}{|y_k|} = a_{kk} - \sum_{\substack{j=1 \\ j \neq k}}^n |a_{kj}| \geq \min_{1 \leq i \leq n} \left(a_{ii} - \sum_{\substack{j=1 \\ j \neq i}}^n |a_{ij}| \right) > 0$$

Similarly, if \mathbf{A} is column diagonally dominant with positive diagonal elements we

need to show that $\frac{\|\mathbf{A}\mathbf{y}\|_1}{\|\mathbf{y}\|_1} \geq \min_{1 \leq j \leq n} \left(a_{jj} - \sum_{\substack{i=1 \\ i \neq j}}^n |a_{ij}| \right) > 0, \forall \mathbf{y} \in \Re^n$. For some arbitrary vector

$\mathbf{y} \in \Re^n$ we have:

$$\begin{aligned} \frac{\|\mathbf{A}\mathbf{y}\|_1}{\|\mathbf{y}\|_1} &= \frac{\sum_{i=1}^n \left| \sum_{j=1}^n a_{ij} y_j \right|}{\sum_{i=1}^n |y_i|} \geq \frac{\sum_{i=1}^n \left(|a_{ii} y_i| - \left| \sum_{\substack{j=1 \\ j \neq i}}^n a_{ij} y_j \right| \right)}{\sum_{i=1}^n |y_i|} \geq \frac{\sum_{i=1}^n \left(|a_{ii} y_i| - \sum_{\substack{j=1 \\ j \neq i}}^n |a_{ij}| |y_j| \right)}{\sum_{i=1}^n |y_i|} \\ &= \frac{\sum_{j=1}^n \left(|a_{jj} y_j| - \sum_{\substack{i=1 \\ i \neq j}}^n |a_{ij}| |y_j| \right)}{\sum_{j=1}^n |y_j|} = \frac{\sum_{j=1}^n \left(|y_j| \left(a_{jj} - \sum_{\substack{i=1 \\ i \neq j}}^n |a_{ij}| \right) \right)}{\sum_{j=1}^n |y_j|} \geq \frac{\left(\sum_{j=1}^n |y_j| \right) \min_{1 \leq j \leq n} \left(a_{jj} - \sum_{\substack{i=1 \\ i \neq j}}^n |a_{ij}| \right)}{\sum_{j=1}^n |y_j|} \\ &= \min_{1 \leq j \leq n} \left(a_{jj} - \sum_{\substack{i=1 \\ i \neq j}}^n |a_{ij}| \right) > 0 \quad \mathbf{Q.E.D.} \end{aligned}$$

Theorem 3. Let $\mathbf{A} = [a_{ij}]$ be a $n \times n$ – row or column – diagonally dominant matrix with positive diagonal elements. If λ is an eigenvalue of \mathbf{A} then $\text{Re } \lambda > 0$.

Proof. This is an immediate consequence of the Gershgorin circle theorem [23], by which every eigenvalue λ_k , $k = 1, \dots, n$ of a square matrix \mathbf{A} is located in one of the n

disks in the complex plane defined by $\left\{ z : |z - a_{ii}| \leq \sum_{\substack{j=1 \\ j \neq i}}^n |a_{ij}| \right\}$, $i = 1, \dots, n$ (i.e. the n

disks centered at a_{ii} and having radius $\sum_{\substack{j=1 \\ j \neq i}}^n |a_{ij}|$, $i = 1, \dots, n$). Obviously, if the matrix \mathbf{A}

is row diagonally dominant with positive diagonal elements, then all Gershgorin disks lie entirely in the positive real semi-plane and thus all eigenvalues of \mathbf{A} have positive

real parts, i.e. $\operatorname{Re} \lambda_k > 0$, $\forall k = 1, \dots, n$. Since the Gershgorin circle theorem can be

restated for the set of disks $\left\{ z : |z - a_{jj}| \leq \sum_{\substack{i=1 \\ i \neq j}}^n |a_{ij}| \right\}$, $j = 1, \dots, n$ (by applying it to \mathbf{A}^T

and because \mathbf{A}, \mathbf{A}^T have the same eigenvalues [24]), it holds again $\operatorname{Re} \lambda_k > 0$, $\forall k = 1, \dots, n$ for the case where \mathbf{A} is column diagonally dominant with positive diagonal elements.

There is an alternative way of proving the theorem. Suppose, to derive a contradiction, that there exists an eigenvalue λ of \mathbf{A} which has $\operatorname{Re} \lambda \leq 0$. Then, if \mathbf{A} is row diagonally dominant with positive diagonal elements it would be

$$|\lambda - a_{ii}| = \sqrt{(a_{ii} + |\operatorname{Re} \lambda|)^2 + (\operatorname{Im} \lambda)^2} > a_{ii} > \sum_{\substack{j=1 \\ j \neq i}}^n |a_{ij}|, \text{ which means that the matrix}$$

$\lambda \mathbf{I} - \mathbf{A}$ is also row diagonally dominant (generally, with complex diagonal elements). However such a matrix is always nonsingular [23], i.e. $\det(\lambda \mathbf{I} - \mathbf{A}) \neq 0$, which contradicts our initial hypothesis that λ is an eigenvalue of \mathbf{A} (a similar proof can be derived for the case of \mathbf{A} being column diagonally dominant with positive diagonal elements). **Q.E.D.**

Theorem 4. If $\mathbf{A} = [a_{ij}]$ is a $n \times n$ – row or column – diagonally dominant matrix with positive diagonal elements then \mathbf{A}^{-1} has only positive diagonal elements.

Proof. Let $\mathbf{A}^{-1} = [\alpha_{ij}]$. For the diagonal elements α_{ii} of \mathbf{A}^{-1} it holds:

$$\alpha_{ii} = (-1)^{i+i} \frac{\det(\mathbf{A}_{ii})}{\det(\mathbf{A})} = \frac{\det(\mathbf{A}_{ii})}{\det(\mathbf{A})}, \quad i = 1, \dots, n$$

where \mathbf{A}_{ii} is the (principal) submatrix of \mathbf{A} obtained by striking out the i th row and the i th column. If \mathbf{A} is – row or column – diagonally dominant with positive diagonal elements, then so is every principal submatrix \mathbf{A}_{ii} , $i = 1, \dots, n$, as is easily verified.

Thus, by Theorem 3 all eigenvalues of \mathbf{A} as well as of any principal submatrix \mathbf{A}_{ii} , $i = 1, \dots, n$ have positive real parts. Let μ_k , $k = 1, \dots, n_r$ and $\gamma_k, \bar{\gamma}_k$, $k = 1, \dots, n_c$ be the –

not necessarily distinct – real and complex eigenvalues of \mathbf{A} respectively (the latter occurring in conjugate pairs), where $n_r + 2n_c = n$. Let also $\mu_k^{(i)}$, $k = 1, \dots, n_r^{(i)}$ and $\gamma_k^{(i)}$, $\bar{\gamma}_k^{(i)}$, $k = 1, \dots, n_c^{(i)}$ denote the real and complex eigenvalues of the principal submatrix \mathbf{A}_{ii} , $i = 1, \dots, n$, where $n_r^{(i)} + 2n_c^{(i)} = n - 1$ for every $i = 1, \dots, n$. Since the determinant of any square matrix is equal to the product of its eigenvalues [24], we arrive at the desired result:

$$\alpha_{ii} = \frac{\det(\mathbf{A}_{ii})}{\det(\mathbf{A})} = \frac{\prod_{k=1}^{n_r^{(i)}} \mu_k^{(i)} \prod_{k=1}^{n_c^{(i)}} \left[(\operatorname{Re} \gamma_k^{(i)})^2 + (\operatorname{Im} \gamma_k^{(i)})^2 \right]}{\prod_{k=1}^{n_r} \mu_k \prod_{k=1}^{n_c} \left[(\operatorname{Re} \gamma_k)^2 + (\operatorname{Im} \gamma_k)^2 \right]} > 0, \quad i = 1, \dots, n \quad \mathbf{Q.E.D.}$$

Theorem 5. If $\mathbf{A} = [a_{ij}]$ is a $n \times n$ row (resp., column) diagonally dominant matrix with positive diagonal elements then the matrix $\mathbf{I} - (\mathbf{I} + \mathbf{A})^{-1} = (\mathbf{I} + \mathbf{A})^{-1} \mathbf{A} = (\mathbf{A}^{-1} + \mathbf{I})^{-1}$ is also row (resp., column) diagonally dominant with positive diagonal elements.

Proof. If \mathbf{A} is row diagonally dominant with positive diagonal elements then clearly the same holds for $\mathbf{I} + \mathbf{A}$. This implies that the inverse $(\mathbf{I} + \mathbf{A})^{-1}$ has only positive diagonal elements (due to Theorem 4) and also satisfies (on account of Theorem 1):

$$\|(\mathbf{I} + \mathbf{A})^{-1}\|_{\infty} < \left[\min_{1 \leq i \leq n} \left(1 + a_{ii} - \sum_{\substack{j=1 \\ j \neq i}}^n |a_{ij}| \right) \right]^{-1} < 1$$

Thus Lemma 2 is applicable and the matrix $\mathbf{I} - (\mathbf{I} + \mathbf{A})^{-1}$ is row diagonally dominant with positive diagonal elements.

Likewise, if \mathbf{A} is column diagonally dominant with positive diagonal elements then so is $\mathbf{I} + \mathbf{A}$, whose inverse $(\mathbf{I} + \mathbf{A})^{-1}$ has only positive diagonal elements and satisfies:

$$\|(\mathbf{I} + \mathbf{A})^{-1}\|_1 < \left[\min_{1 \leq j \leq n} \left(1 + a_{jj} - \sum_{\substack{i=1 \\ i \neq j}}^n |a_{ij}| \right) \right]^{-1} < 1$$

Thus it follows that the matrix $\mathbf{I} - (\mathbf{I} + \mathbf{A})^{-1}$ is column diagonally dominant with positive diagonal elements. **Q.E.D.**

Corollary 1. If $\mathbf{A} = [a_{ij}]$ is a $n \times n$ row (resp., column) diagonally dominant matrix with positive diagonal elements and $\mathbf{D} = [d_i]$ is a $n \times n$ positive diagonal matrix, then the matrix $(\mathbf{A}^{-1} + \mathbf{D})^{-1} = (\mathbf{I} + \mathbf{AD})^{-1} \mathbf{A}$ is also row (resp., column) diagonally dominant with positive diagonal elements.

Proof. If \mathbf{A} is a row diagonally dominant matrix with positive diagonal elements and \mathbf{D} is a positive diagonal matrix, then by successive use of Lemma 1, Theorem 5, and again Lemma 1 we have that the matrices \mathbf{DA} , $((\mathbf{DA})^{-1} + \mathbf{I})^{-1}$, and $\mathbf{D}^{-1}((\mathbf{DA})^{-1} + \mathbf{I})^{-1} = (\mathbf{A}^{-1} + \mathbf{D})^{-1}$ are also row diagonally dominant with positive diagonal elements.

In a similar manner, if \mathbf{A} is column diagonally dominant with positive diagonal elements, then the matrices \mathbf{AD} , $((\mathbf{AD})^{-1} + \mathbf{I})^{-1}$, and $((\mathbf{AD})^{-1} + \mathbf{I})^{-1} \mathbf{D}^{-1} = (\mathbf{A}^{-1} + \mathbf{D})^{-1}$ are also column diagonally dominant with positive diagonal elements. **Q.E.D.**

Theorem 6. If $\mathbf{A} = [a_{ij}]$ is a $n \times n$ – row or column – diagonally dominant matrix with positive diagonal elements, then for the matrix $\mathbf{B} = (\mathbf{I} + \mathbf{A})^{-1}$ it holds $\lim_{N \rightarrow \infty} \mathbf{B}^N = \mathbf{0}$.

Proof. It is well known [23] that a sufficient condition to have $\lim_{N \rightarrow \infty} \mathbf{B}^N = \mathbf{0}$ is either $\|\mathbf{B}\|_\infty < 1$ or $\|\mathbf{B}\|_1 < 1$, which for $\mathbf{B} = (\mathbf{I} + \mathbf{A})^{-1}$ follows directly from Theorem 1 when \mathbf{A} is – row or column – diagonally dominant with positive diagonal elements.

As an alternative proof, it is also well known [23] that $\lim_{N \rightarrow \infty} \mathbf{B}^N = \mathbf{0}$ if and only if

$\rho(\mathbf{B}) = \max_{1 \leq k \leq n} |\lambda_k(\mathbf{B})| < 1$, where $\lambda_k(\mathbf{B})$, $k = 1, \dots, n$ are the – not necessarily distinct – eigenvalues of \mathbf{B} and $\rho(\mathbf{B})$ is the largest of their magnitudes (called the *spectral radius* of \mathbf{B}). Also, for $\mathbf{B} = (\mathbf{I} + \mathbf{A})^{-1}$ it is true that $\lambda_k(\mathbf{B}) = \frac{1}{1 + \lambda_k(\mathbf{A})}$, $k = 1, \dots, n$ [24].

If \mathbf{A} is – row or column – diagonally dominant with positive diagonal elements, then it follows from Theorem 3 that $\operatorname{Re} \lambda_k(\mathbf{A}) > 0$, $\forall k = 1, \dots, n$. This gives:

$$|\lambda_k(\mathbf{B})| = \frac{1}{|1 + \lambda_k(\mathbf{A})|} = \frac{1}{\sqrt{(1 + \operatorname{Re} \lambda_k(\mathbf{A}))^2 + (\operatorname{Im} \lambda_k(\mathbf{A}))^2}} < 1, \quad \forall k = 1, \dots, n,$$

or finally $\rho(\mathbf{B}) < 1$. **Q.E.D.**

APPENDIX B

MATLAB CODE

B.1 Minimize area

B.1.1 Create waveforms for currents of the input file and find current nodes and voltage nodes

```
load c1355_5000.txt %input data file
idc=c1355_5000; %currents in A
nms=size(idc,1); %size of input data

T=1e-9; %clock period in s
N=10; %number of sampling points
h=T/N; %sampling step

t1=(1:N/2)*h; %first half of period
itri1=2*idc*t1/T;
iwav1=itri1;
t2=(N/2+1:N)*h; %second half of period
itri2=2*idc*(N*T-T+2*t2-N*t2)/(N*T);
iwav2=itri2;
t=[t1 t2];
iwav=[iwav1 iwav2];

n1=10; %number of vertical lines in the grid
n2=10; %number of horizontal lines in the grid
vn=6; %number of voltage nodes in the grid
sn=5; %number of current sinks
isn =[56 45 18 93 6];
ivn =[52 60 23 75 2 19];
```

B.1.2 Find movement vector and maximal points

```
nm=3000; %size of main sample
off=2000; %number of extra samples (offset) in input data
%number of sampling points (N) in a clock period must already
%be defined
mvarsam=zeros(nm,N*sn);
for i=1:sn
    mvarsam(:,N*(i-1)+1:N*i)=iwav(off*i+nm*(i-
1)+1:off*i+nm*i,:); %create multivariate sample (array of
                        %current waveforms must already exist)
end

n=30; %size of sub-samples for estimation (must be at least
      %30)
m=nm/n; %number of sub-samples - or size of sample of maxima -
        %for estimation (must be at least 100)

%+-----+%
%| Statistical maxima estimation |%
%+-----+%

xm=zeros(m,1);
eulg=0.5772; %Euler gamma constant
den=1/(1+n*sqrt(pi*log(n))*(erf(sqrt(log(n)))-1));
%denominator of estimate

stmat=zeros(2,N*sn);
for i=1:N*sn
    sam=mvarsam(:,i);
    smax=max(sam);
    for j=1:m
        xm(j)=max(sam(n*(j-1)+1:n*j)); %sample of maxima
    end
end
```

```

        bg=std(xm)*sqrt(6)/pi;
        ag=mean(xm)-bg*eulg;
        wg=ag+bg*den; %upper endpoint estimate
        stmat(:,i)=[smax;wg];
    end

    mov=stmat(2,:)-stmat(1,:); %movement vector for the sample
                                %maximal points

    %+-----+%
    %| Calculation of worst-case current vectors      |%
    %+-----+%

    %locate maximal points of the sample space
    mmal=[];
    for i=1:nm
        mmali=mvarsam(i,:);
        comp=(repmat(mmal,i,nm,1)<mvarsam);
        comp2=(sum(comp,2)==N*sn);
        if sum(comp2)==0
            mmal=[mmal;mmali];
        end
    end
    nmal=size(mmal,1);

    iex=mmal+repmat(mov,nmal,1); %statistically project sample
                                %maximal points into the whole population

    %alternative configuration of array of maximal points
    ialt=zeros(nmal,N*sn);
    for j=1:N
        for i=1:sn
            ialt(:,(j-1)*sn+i)=iex(:,N*(i-1)+j);
        end
    end
end

```

```

%MEC excitations (in alternative configuration) for
%pessimistic analysis
ialt_pes=zeros(1,N*sn);
for j=1:N
    for i=1:sn
        ialt_pes(:,(j-1)*sn+i)=stmat(2,N*(i-1)+j);
    end
end
end

```

B.1.3 Constraint function (gconstr)

Create and analyze the power grid

```

function [c,ceq]=gconstr(x,ialt,co,ivn,isn,idec)

rsh=co(1);
rsv=co(2);
lsh=co(3);
lsv=co(4);
vo=co(5);
n1=co(8);
n2=co(9);
pv=co(10);
ph=co(11);
vn=co(12);
cffh=co(13);
cffv=co(14);
cpvh=co(15);
cppv=co(16);
cox=co(17);
lpin=co(19);
rpin=co(20);
cpin=co(21);
sn=co(22);
N=co(24);
h=co(25);

```

```

ndec=co(26);
hsub=co(27);

%-----%

%capacitance and incidence matrix
ch= repmat(cpph*pv*x(1:n2,:)+cffh*pv,1,n1-1); %horizontal
                                     %branch capacitances
cv= repmat(cppv*ph*x(n2+1:n2+n1,:)+cffv*ph,1,n2-1); %vertical
                                     %branch capacitances

C=zeros(n1*n2,n1*n2);
A1=zeros(n1*n2,n1*(n2-1)+n2*(n1-1)+vn);

%enumerate horizontal branches
for i=1:n2
    for j=1:n1-1
        ni1=(i-1)*n1+j; %node indices for current branch
        ni2=ni1+1;
        ni3=(i-1)*(n1-1)+j; %branch index conversion from 2D
                               %to 1D
        C(ni1,ni1)=C(ni1,ni1)+(1/2)*ch(i,j);
        C(ni2,ni2)=C(ni2,ni2)+(1/2)*ch(i,j);
        A1(ni1,ni3)=1;
        A1(ni2,ni3)=-1;
    end
end

%enumerate vertical branches
for i=1:n1
    for j=1:n2-1
        ni1=(j-1)*n1+i; %node indices for current branch
        ni2=ni1+n1;
        ni3=(i-1)*(n2-1)+j+n2*(n1-1); %branch index conversion
                                         %from 2D to 1D
        C(ni1,ni1)=C(ni1,ni1)+(1/2)*cv(i,j);
        C(ni2,ni2)=C(ni2,ni2)+(1/2)*cv(i,j);
    end
end

```

```

        Al(ni1,ni3)=1;
        Al(ni2,ni3)=-1;
    end
end

%enumerate supply branches
for i=1:vn
    C(ivn(i),ivn(i))=C(ivn(i),ivn(i))+cpin;
    Al(ivn(i),n1*(n2-1)+n2*(n1-1)+i)=-1;
end

%enumerate decoupling capacitors
cdec=cox;
for i=1:ndec
    C(idec(i),idec(i))=C(idec(i),idec(i))+cdec*x(n2+n1+i).^2;
end

%-----%

%inductance matrix
lh=repmat(lsh*pv*log(8*hsub./x(1:n2,:)),1,n1-1);
%horizontal branch inductances
lv=repmat(lsv*ph*log(8*hsub./x(n2+1:n2+n1,:)),1,n2-1);
%vertical branch inductances

lbranch=[reshape(lh',n2*(n1-1),1);reshape(lv',n1*(n2-1),1);lpin*ones(vn,1)];

L=diag(lbranch);

%-----%

%resistance matrix
rh=repmat(rsh*pv./x(1:n2,:),1,n1-1); %horizontal branch
                                %resistances
rv=repmat(rsv*ph./x(n2+1:n2+n1,:),1,n2-1);

```

```

%vertical branch resistances
rbranch=[reshape(rh',n2*(n1-1),1);reshape(rv',n1*(n2-
1),1);rpin*ones(vn,1)];
R=diag(rbranch);

%-----%

%transient analysis for maximal waveform excitations
Gb=[zeros(n1*n2,n1*n2) A1;A1' -R];
Cb=[C zeros(n1*n2,n1*(n2-1)+n2*(n1-1)+vn);zeros(n1*(n2-
1)+n2*(n1-1)+vn,n1*n2) -L];

D=inv(Gb+Cb/h);
B=D*Cb/h;

nialt=size(ialt,1);
Is=zeros(n1*n2+n1*(n2-1)+n2*(n1-1)+vn,nialt);
%current excitations from gates
Vb=zeros(n1*n2+n1*(n2-1)+n2*(n1-1)+vn,nialt);
%node voltages and branch currents
Vmean=zeros(n1*n2,nialt);

for j=1:N
    Is(isn,:)=ialt(:,sn*(j-1)+1:sn*j)';
    Vb=D*Is+B*Vb;
    Vmean=Vmean+Vb(1:n1*n2,:);
end
Vmean=Vmean/N;

Vm=max(Vmean,[],2); %maximum voltage drops (in V)
Vms=Vm(isn,:); %voltage drops at sinks
c=Vms-vo;
ceq=[];

```

B.1.4 Objective function (gridarea)

Calculate area

```
function a=gridarea(x,ialt,co,ivn,isn,idec)
sizv=co(6);
sizh=co(7);
n1=co(8);
n2=co(9);
ndec=co(26);
a=sizh*sum(x(1:n2,:))+sizv*sum(x(n2+1:n2+n1,:))+
sum(x(n2+n1+1:n2+n1+ndec,:).^2);
```

B.1.5 Initialization of the variables and optimization of the grid

```
%+-----+%
%| Grid setup    |%
%+-----+%

%Optimization code starts here
rsh=1e-1; %horizontal sheet resistance (in Ohms/sq)
rsv=1e-1; %vertical sheet resistance (in Ohms/sq)
lsh=2e-7; %horizontal inductance per unit length (in H/m)
lsv=2e-7; %vertical inductance per unit length (in H/m)
vo=0.1;   %voltage drop tolerance
sizv=350e-6; %vertical size of chip (in m)
sizh=350e-6; %horizontal size of chip (in m)
pv=sizh/(n1-1); %pitch of vertical lines
ph=sizv/(n2-1); %pitch of horizontal lines
cffh=1e-10;    %horizontal cff capacity (in F/m)
cffv=1e-10;    %vertical cff capacity (in F/m)
cpph=1e-4;     %horizontal cpp capacity (in F/m^2)
cppv=1e-4;     %vertical cpp capacity (in F/m^2)
cox=14.16e-3;  %eox/tox (in F/m^2)
hsub=18.75e-6; % (150e-6)/8
hd=10e-6;      %height of decoups (in m)
lpin=1e-10;    %pin inductance (in H)
```



```

rpin=1e3;          %Vdd pin resistance in Ohms
cpin=10e-12;      %pin capacitance in F

% -> (n1 x n2) nodes in the grid (including voltage nodes)
idec=[1:n1*n2];
ndec=size(idec,2); %%number of decaps used

co=[rsh rsv lsh lsv vo sizv sizh n1 n2 pv ph vn cffh cffv cpph
cppv cox hd lpin rpin cpin sn T N h ndec hsub];

winit=ones(n2+n1,1)*1e-6;
wlb=0.4*ones(n2+n1,1)*1e-6;
wub=ones(n2+n1,1);
wub(1:n2,:)=ph;    %taking into account the pitch of
                    %horizontal lines
wub(n2+1:n2+n1,:)=pv;%taking into account the pitch of
                    %vertical lines

linit=250*ones(ndec,1)*1e-6;
llb=0.4*ones(ndec,1)*1e-6;
lub=ones(ndec,1);  %taking into account the horizontal
                    %size of chip

xinit=[winit; linit];
xlb=[wlb; llb];
xub=[wub; lub];
options=optimset('Algorithm','active-set','Display','iter');

[xeff,areff,exitflag]=fmincon(@gridarea,xinit,[],[],[],[],xlb,
xub,@gconstr,options,ialt,co,ivn,isn,idec);

exitflag
areff

%%area of wires
war=sizh*sum(xeff(1:n2,:))+sizv*sum(xeff(n2+1:n2+n1,:))

```

```

%%area of decaps
dar=sum(xeff(n2+n1+1:n2+n1+ndec,:).^2)
%evaluate constraints at the final solution
geff=gconstr(xeff,ialt,co,ivn,isn,idec);

[xpes,arpes,flagpes]=fmincon(@gridarea,xinit,[],[],[],[],xlb,x
ub,@gconstr,options,ialt_pes,co,ivn,isn,idec);

flagpes
arpes

%%area of wires
pwar=sizh*sum(xpes(1:n2,:))+sizv*sum(xpes(n2+1:n2+n1,:))
%%area of decaps
pdar=sum(xpes(n2+n1+1:n2+n1+ndec,:).^2)
%evaluate constraints at the final solution
gpes=gconstr(xpes,ialt,co,ivn,isn,idec);

perc=100*(arpes-areff)/areff
percw=100*(pwar-war)/war
percd=100*(pdar-dar)/dar
xeff

my=geff+vo
myp=gpes+vo

```

B.2 Minimize noise (Voltage drop)

B.2.1 Create waveforms for currents of the input file and find current nodes and voltage nodes

```

load c7552_4002.txt %input data file
idc=c7552_4002; %currents in A
nms=size(idc,1); %size of input data

```

```

T=1e-9; %clock period in s
N=10; %number of sampling points
h=T/N; %sampling step

t1=(1:N/2)*h; %first half of period
itri1=2*idc*t1/T;
iwav1=itri1;
t2=(N/2+1:N)*h; %second half of period
itri2=2*idc*(N*T-T+2*t2-N*t2)/(N*T);
iwav2=itri2;
t=[t1 t2];
iwav=[iwav1 iwav2];

n1=20; %number of vertical lines in the grid
n2=20; %number of horizontal lines in the grid
vn=15; %number of voltage nodes in the grid
sn=42; %number of current sinks

isn=[2 10 18 31 49 56 57 65 79 86 89 107 128 140 143 145 146
152 164 174 176 180 237 243 260 264 273 281 287 290 293 314
339 341 352 357 359 363 378 386 395 397]
ivn=[16 30 34 38 63 67 81 96 98 149 159 277 351 370 376]

```

B.2.2 Find movement vector and maximal points

```

nm=3000; %size of main sample
off=1002; %number of extra samples (offset) in input data

mvarsam=zeros(nm,N*sn);
for i=1:sn
    mvarsam(:,N*(i-1)+1:N*i)=iwav(off*i+nm*(i-1)+1:off*i+nm*i,:);
end

```

```

n=30; %size of sub-samples for estimation (must be at least
30)
m=n*m/n; %number of sub-samples - or size of sample of maxima -
for estimation (must be at least 100)

%+-----+%
%| Statistical maxima estimation |%
%+-----+%

xm=zeros(m,1);

eulg=0.5772; %Euler gamma constant
den=1/(1+n*sqrt(pi*log(n))*(erf(sqrt(log(n)))-1));
%denominator of estimate
stmat=zeros(2,N*sn);

for i=1:N*sn
    sam=mvarsam(:,i);
    smax=max(sam);

    for j=1:m
        xm(j)=max(sam(n*(j-1)+1:n*j)); %sample of maxima
    end

    bg=std(xm)*sqrt(6)/pi;
    ag=mean(xm)-bg*eulg;
    wg=ag+bg*den; %upper endpoint estimate

    stmat(:,i)=[smax;wg];
end

mov=stmat(2,:)-stmat(1,:);
%movement vector for the sample maximal points

```

```

%+-----+%
%| Calculation of worst-case current vectors |%
%+-----+%

%locate maximal points of the sample space
mmal=[];
for i=1:nm
    mmali=mvarsam(i,:);
    comp=(repmat(mmali,nm,1)<mvarsam);
    comp2=(sum(comp,2)==N*sn);
    if sum(comp2)==0
        mmal=[mmal;mmali];
    end
end
nmal=size(mmal,1);

iex=mmal+repmat(mov,nmal,1); %statistically project sample
                             %maximal points into the whole population

%alternative configuration of array of maximal points
ialt=zeros(nmal,N*sn);
for j=1:N
    for i=1:sn
        ialt(:,(j-1)*sn+i)=iex(:,N*(i-1)+j);
    end
end

%MEC excitations (in alternative configuration) for
%pessimistic analysis
ialt_pes=zeros(1,N*sn);
for j=1:N
    for i=1:sn
        ialt_pes(:,(j-1)*sn+i)=stmat(2,N*(i-1)+j);
    end
end
end

```

B.2.3 Objective function (gridnoise)

Create and analyze the power grid

```
function [a b]=gridnoise(x,ialt,co,ivn,isn,idec)
rsh=co(1);
rsv=co(2);
lsh=co(3);
lsv=co(4);
vo=co(5);
n1=co(8);
n2=co(9);
pv=co(10);
ph=co(11);
vn=co(12);
cffh=co(13);
cffv=co(14);
cpph=co(15);
cppv=co(16);
cox=co(17);
lpin=co(19);
rpin=co(20);
cpin=co(21);
sn=co(22);
N=co(24);
h=co(25);
ndec=co(26);
hsub=co(27);

%-----%
%capacitance and incidence matrix

ch=repmat(cpph*pv*x(1:n2,:)+cffh*pv,1,n1-1);
%horizontal branch capacitances
cv=repmat(cppv*ph*x(n2+1:n2+n1,:)+cffv*ph,1,n2-1);
%vertical branch capacitances
```

```

C=zeros(n1*n2,n1*n2);
Al=zeros(n1*n2,n1*(n2-1)+n2*(n1-1)+vn);

%enumerate horizontal branches
for i=1:n2
    for j=1:n1-1
        ni1=(i-1)*n1+j; %node indices for current branch
        ni2=ni1+1;
        ni3=(i-1)*(n1-1)+j; %branch index conversion from 2D
                                %to 1D
        C(ni1,ni1)=C(ni1,ni1)+(1/2)*ch(i,j);
        C(ni2,ni2)=C(ni2,ni2)+(1/2)*ch(i,j);
        Al(ni1,ni3)=1;
        Al(ni2,ni3)=-1;
    end
end

%enumerate vertical branches
for i=1:n1
    for j=1:n2-1
        ni1=(j-1)*n1+i; %node indices for current branch
        ni2=ni1+n1;
        ni3=(i-1)*(n2-1)+j+n2*(n1-1);
        %branch index conversion from 2D to 1D
        C(ni1,ni1)=C(ni1,ni1)+(1/2)*cv(i,j);
        C(ni2,ni2)=C(ni2,ni2)+(1/2)*cv(i,j);
        Al(ni1,ni3)=1;
        Al(ni2,ni3)=-1;
    end
end

%enumerate supply branches
for i=1:vn
    C(ivn(i),ivn(i))=C(ivn(i),ivn(i))+cpin;
    Al(ivn(i),n1*(n2-1)+n2*(n1-1)+i)=-1;
end

```

```

%enumerate decoupling capacitors
cdec=cox;
for i=1:ndec
    C(idec(i),idec(i))=C(idec(i),idec(i))+cdec*x(n2+n1+i).^2;
end

%-----%
%inductance matrix
lh=repmat(lsh*pv*log(8*hsub./x(1:n2,:)),1,n1-1);
%horizontal branch inductances
lv=repmat(lsv*ph*log(8*hsub./x(n2+1:n2+n1,:)),1,n2-1);
%vertical branch inductances

lbranch=[reshape(lh',n2*(n1-1),1);reshape(lv',n1*(n2-
1),1);lpin*ones(vn,1)];

L=diag(lbranch);

%-----%
%resistance matrix
rh=repmat(rsh*pv./x(1:n2,:),1,n1-1); %horizontal branch
                                %resistances
rv=repmat(rsv*ph./x(n2+1:n2+n1,:),1,n2-1);
%vertical branch resistances
rbranch=[reshape(rh',n2*(n1-1),1);reshape(rv',n1*(n2-
1),1);rpin*ones(vn,1)];
R=diag(rbranch);

%-----%
%transient analysis for maximal waveform excitations
Gb=[zeros(n1*n2,n1*n2) A1;A1' -R];
Cb=[C zeros(n1*n2,n1*(n2-1)+n2*(n1-1)+vn);zeros(n1*(n2-
1)+n2*(n1-1)+vn,n1*n2) -L];

```



```

D=inv(Gb+Cb/h);
B=D*Cb/h;

nialt=size(ialt,1);
Is=zeros(n1*n2+n1*(n2-1)+n2*(n1-1)+vn,nialt);
%current excitations from gates
Vb=zeros(n1*n2+n1*(n2-1)+n2*(n1-1)+vn,nialt);
%node voltages and branch currents
Vmean=zeros(n1*n2,nialt);

for j=1:N
    Is(isn,:)=ialt(:,sn*(j-1)+1:sn*j)';
    Vb=D*Is+B*Vb;
    Vmean=Vmean+max(Vb(1:n1*n2,:)-vo,zeros(n1*n2,nialt));
end

Vm=max(Vmean,[],2); %maximum voltage drops (in V)
a=sum(Vm); %voltage drops at sinks
b=(Vm>eps);

```

B.2.4 Initialization of the variables and optimization of the grid

```

%+-----+%
%| Grid setup   |%
%+-----+%
%Optimization code starts here
rsh=1e-1; %horizontal sheet resistance (in Ohms/sq)
rsv=1e-1; %vertical sheet resistance (in Ohms/sq)
lsh=2e-7; %horizontal inductance per unit length (in H/m)
lsv=2e-7; %vertical inductance per unit length (in H/m)
vo=0.1; %voltage drop tolerance
sizv=350e-6; %vertical size of chip (in m)
sizh=350e-6; %horizontal size of chip (in m)
pv=sizh/(n1-1); %pitch of vertical lines
ph=sizv/(n2-1); %pitch of horizontal lines
cffh=1e-10; %horizontal cff capacity (in F/m)

```

```

cffv=1e-10;      %vertical cff capacity (in F/m)
cpph=1e-4;      %horizontal cpp capacity (in F/m^2)
cppv=1e-4;      %vertical cpp capacity (in F/m^2)
cox=14.16e-3;   %eox/tox (in F/m^2)
hsub=18.75e-6;  %(150e-6)/8
hd=10e-6;       %height of decoups (in m)
lpin=1e-10;     %pin inductance (in H)
rpin=1e3;       %Vdd pin resistance in Ohms
cpin=10e-12;    %pin capacitance in F
% -> (n1 x n2) nodes in the grid (including voltage nodes)
idec=[1:n1*n2];
ndec=size(idec,2); %%number of decaps used

co=[rsh rsv lsh lsv vo sizv sizh n1 n2 pv ph vn cffh cffv cpph
cppv cox hd lpin rpin cpin sn T N h ndec hsub];

winit=ones(n2+n1,1)*1e-6;
wlb=0.4*ones(n2+n1,1)*1e-6;
wub=ones(n2+n1,1);
wub(1:n2,:)=ph;    %taking into account the pitch of
                    %horizontal lines
wub(n2+1:n2+n1,:)=pv;%taking into account the pitch of
                    %vertical lines

linit=30*ones(ndec,1)*1e-6;
llb=0.4*ones(ndec,1)*1e-6;
lub=ones(ndec,1)*1e-5;%taking into account the horizontal size
                    %of chip

xinit=[winit; linit];
xlb=[wlb; llb];
xub=[wub; lub];
options=optimset('Algorithm','active-set','Display','iter');

[xeff,noiseff,exitflag]=fmincon(@gridnoise,xinit,[],[],[],[],x
lb,xub,[],options,ialt,co,ivn,isn,idec);

```

```

exitflag
noiseff

[xpes,noisepes,flagpes]=fmincon(@gridnoise,xinit,[],[],[],[],x
lb,xub,[],options,ialt_pes,co,ivn,isn,idec);
flagpes
noisepes
perc=100*(noisepes-noiseff)/noiseff

xeff
[a b]=gridnoise(xeff,ialt,co,ivn,isn,idec);
a
s=sum(b)

```

REFERENCES

- [1] A. Dharchoudhury, R. Panda, D. Blaauw, R. Vaidyanathan, B. Tutuianu, and D. Bearden, “Design and analysis of power distribution networks in PowerPC microprocessors”, *ACM/IEEE Design Automation Conf.*, 1998.
- [2] G. Steele, D. Overhauser, S. Rochel, and S. Hussain, “Full-chip verification methods for DSM power distribution systems”, *ACM/IEEE Design Automation Conf.*, 1998.
- [3] X. Tan, C. Shi, D. Lungeanu, J. Lee, and L. Yuan, “Reliability-constrained optimization of VLSI power/ground networks via sequence of linear programmings”, *ACM/IEEE Design Automation Conf.*, 1999.
- [4] T. Wang and C. Chen, “Optimization of the power/ground network wire-sizing and spacing based on sequential network simplex algorithm”, *IEEE Int. Symp. Quality Electronic Design*, 2002.
- [5] X. Tan and C. Shi, “Efficient very large scale integration power/ground network sizing based on equivalent circuit modeling”, *IEEE Trans. Computer-Aided Design*, vol. 22, pp. 277-284, 2003.
- [6] S. Chowdhury, “Optimum design of reliable IC power networks having general graph topologies”, *ACM/IEEE Design Automation Conf.*, 1989.
- [7] H. Royden, *Real Analysis*, 3rd ed., Prentice-Hall, 1988.
- [8] R. Horn and C. Johnson, *Matrix Analysis*, Cambridge, 1990.
- [9] A. Ruehli (ed.), *Circuit Analysis, Simulation and Design*, North-Holland, 1986.
- [10] A. Berman and R. Plemmons, *Nonnegative Matrices in the Mathematical Sciences*, Academic Press, 1979.

- [11] Y. Saad, *Iterative Methods for Sparse Linear Systems*, 2nd ed., SIAM, 2003.
- [12] H. Ji, A. Devgan, and W. Dai, “KSim: A stable and efficient RKC simulator for capturing on-chip inductance effect”, *ACM/IEEE Asia & South Pacific Design Automation Conf.*, 2001.
- [13] N. Evmorfopoulos, G. Stamoulis, J. Avaritsiotis, “A Monte Carlo approach for maximum power estimation based on extreme value theory ”, *IEEE Trans. Computer-Aided Design*, Vol 21, pp. 415-432, 2002.
- [14] H. Kung, F. Luccio, and F. Preparata, “On finding the maxima of a set of vectors”, *J. ACM*, vol. 22, pp. 469-476, 1975.
- [15] N. Evmorfopoulos, D. Karampatzakis, G. Stamoulis, “Precise Identification of the Worst-Case Voltage Drop Conditions in Power Grid Verification”, *ACM/IEEE Int. Conf. Computer-Aided Design*, 2006.
- [16] S. W. Director and R. A. Rohrer. ‘The Generalized Adjoint Network and Network Sensitivities’. *IEEE Trans. on Circuit Theory*, Vol. 16 , Issue 3, 318 – 323, August 1969.
- [17] P. Gill, W. Murray, M. Saunders, “SNOPT: An SQP algorithm for large-scale constrained optimization”, *SIAM Review*, Vol. 47, No. 1, pp. 99-131, 2005.
- [18] P. T. Boggs and J. W. Tolle. *Sequential Quadratic Programming*. Cambridge Univ. Press, Cambridge, 1995.
- [19] H. Kriplani, F. Najm, and I. Hajj, “Pattern independent maximum current estimation in power and ground buses of CMOS VLSI circuits: algorithms, signal correlations and their resolution”, *IEEE Trans. Computer-Aided Design*, vol. 14, pp. 998-1012, 1995.
- [20] H. Su, J. Hu, S. Sapatnekar, S. Nasif, “A Methodology for the Simultaneous

Design of Supply and Signal Networks”, *IEEE Trans. on Computer-Aided Design*, Vol. 23, Issue 12, pp. 1614 – 1624, 2004.

[21] H. Su, S. Sapatnekar, S. Nasif, “Optimal Decoupling Capacitor Sizing and Placement for Standard Cell Layout Designs”, *IEEE Trans. on Computer-Aided Design*, Vol. 22 , Issue 4, pp. 428 - 436, 2003.

[22] H. Su, K. Gala, S. Sapatnekar, “Analysis and Optimization of Structured Power/Ground Networks”, *IEEE Trans. on Computer-Aided Design*, Vol. 22 , Issue 11, 1533 – 1544, 2003.

[23] Y. Saad, *Iterative Methods for Sparse Linear Systems*, 2nd ed., SIAM, 2003.

[24] R. Horn and C. Johnson, *Matrix Analysis*, Cambridge, 1990.